A MULTI-TRACER STUDY OF THE ORIGINS, SYSTEMATICS AND HYDROLOGICAL LINKAGES OF HIGH NITRATE CONCENTRATIONS IN GROUND WATER IN BOCHUM DISTRICT, LIMPOPO PROVINCE

Report to the

WATER RESEARCH COMMISSION

by

B. Th. Verhagen
School of Geosciences, University of the Witwatersrand, Johannesburg

M.J. Butler
Environmental Isotope Group, iThemba LABS (Gauteng), Johannesburg

E. van Wyk
Department of Water Affairs and Forestry, Pretoria

S. Mutheiwana
Department of Water Affairs and Forestry, Polokwane

WRC Report No. 1328/1/09
ISBN 978-1-77005-755-6

March 2009

DISCLAIMER

This report has been reviewed by the Water Research Commission (WRC) and approved for publication. Approval does not signify that the contents necessarily reflect the views and policies of the WRC, nor does mention of trade names or commercial products constitute endorsement or recommendation for use

EXECUTIVE SUMMARY

Ground water in Limpopo Province of South Africa is characterised by the wide spread occurrence of high nitrate concentrations which were generally accepted to be of anthropogenic origin. In a ground water resource study in the Taaibosch Karoo graben, part of an International Atomic Energy Agency regional study, environmental isotope, hydrochemical and hydrogeological suggested a model for the natural production of high nitrate concentrations in a basalt aquifer. This was investigated further under a WRC contract, which foresaw a second phase in a different (hydro)geological environment. The area chosen was Bochum, with numerous rural villages, underlain by metamorphic granite and sandstone. Two sets of samples were taken from boreholes equipped with either hand pumps or motorised pumps that were analysed for major ion chemistry and both stable and radioactive isotopes.

The ground water from both the crystalline and sedimentary aquifers at Bochum was found to be quite recent showing none of the older component and mixtures that characterises the Taaibosch area, conforming to the model for a phreatic aquifer with shallow fracture development. The stable isotopes show similar rainfall selectivity of recharge as at Taaibosch, but without evaporative enrichment due to ponding. Hydrochemical development shows distinctive differences between the two aquifer groups with an absence of ion exchange, already suggested by the carbon-13/carbon-14 relationship. The trend is from an initial expected Ca,Mg-HCO_3 dominance to a more Na, Cl and SO_4 mineralised type. An incidence of high NO_3 values similar to Taaibosch was observed.

Nitrate concentrations show an increase with increasing ground water residence time but not with mineralisation, suggesting sub-surface production. The increase of Si with increasing NO_3 that characterises Taaibosch is absent. There appears also to be no correlation with the aquifer environment. Nitrogen isotope ratios that may be diagnostic of anthropogenic pollution show no correlation with nitrate concentration, but a pronounced dependence on the dissolved oxygen in ground water. This is ascribed to dentrification that may in turn indicate widespread presence of dissolved organic carbon. An extreme case of sewage pollution in a borehole shows complete denitrification. These observations caution against simply regarding nitrate concentrations as a measure of pollution.

We conclude from this study that although high nitrate concentrations at Bochum have an anthropogenic component, the natural, tree-root driven process may also contribute. This particular and pronounced process may well be a characteristic of basalt aquifers in general. The study has shown that isotopic information is essential in understanding the hydrological and chemical processes that underlie phenomena such as nitrate development. It is recommended that isotope studies be more widely applied in hydrogeology; that a reliable, routine facility for nitrogen isotope analysis in water be established and that the occurrence of nitrate in (Karoo) basalt aquifers, such as underlying the Springbok Flats, be re-visited.

TABLE OF CONTENTS

LIST OF FIGURES

LIST OF TABLES

1. INTRODUCTION

The origin of nitrate in ground water in southern Africa, especially at higher concentrations that impair potability, has been the subject of numerous studies (e.g. Heaton 1984, 1985; Stadler 2006; Talma and Tredoux 2005; Tredoux 1993; Taussig and Verhagen 1991). The general opinion has been that higher concentrations that exceed potability limits are probably of anthropogenic origin, over and above natural production. Because of the complexity of processes leading to the formation of nitrate in ground water, origins cannot be readily established. Results obtained in the course of a ground water resource investigation in the Taaibosch area of Limpopo Province (IAEA 2002), lead to a model for the formation of high nitrate levels by natural processes.

The area chosen was at Bochum, south of the Blouberg, which is underlain by metamorphic granites and sandstone and is referred to as Phase II of the project. Phase I was conducted within the Taaibosch area and the results are shown in Appendix 1.

2. STUDY AREA

2.1 Motivation

The Bochum project was aimed at investigating the sources of high nitrate levels in the Taaibosch area, Bochum, Limpopo Province.

Sampling mainly unequipped boreholes for this study requires major field equipment and is largely dependent on the cooperation of DWAF. A series of samples was obtained in March 2007, mainly from exploration boreholes drilled the in deeper sandstone aquifer underlying basalt in the Taaibosch area as an outcome of the earlier resource investigation. This work was aimed at extending the characterization of the deep aquifer, which should contribute towards devising an integrated, conjunctive exploitation model of this high quality, potentially regional resource. The construction of such a model, and further research in support thereof, is the subject of a PhD project (M.J. Butler).

The isotope data obtained from the March 2007 sample suite, along with field observations, are presented in Table 1. Several of the deep wells sampled had been sampled several years previously. The radiocarbon data has remained largely unchanged. This was to be expected, as neither significant exploitation nor significant recharge events had occurred in the interim.

It was found that high nitrate levels, ubiquitous in Limpopo Province, are not necessarily associated with anthropogenic sources in the Taaibosch study area. Various hydrogeological, hydrochemical and environmental isotope linkages gave rise to a model of nitrate production involving phreatophyte roots (Verhagen et al. 2004a,b). This is probably associated also with hydrological, hydrochemical and biological processes in the conditions peculiar to the basalt aquifer. An area around the settlement of Bochum, to the south of the Blouberg, was selected for the extension of this study (Figure 1). The study area is underlain by two contrasting hydrogeological regimes: metamorphic granites and sandstones.

Table 1: Isotope and borehole data for Phase 1 (Taaibosch) study, 12-15 March 2007.

Lab No.	Sample ID	^{14}C (pMC) 2007	Radon (CPMa)	δD (‰)	δ^{18}O (‰)	δ^{13}C (‰)	^{3}H (T.U.)	^{14}C (pMC) 2001-2003	Radon (CPMa)	Water Level (m)	Bh Depth (m)	Strike (m)	Yield (l/s)	Geology
TT 162	H26-0467	66.8 ±1.8	22.4	-30.9	-4.62	-9.78	0.1 ±0.2	75.1 ±1.9	0.0	27.9	150	75; 95	1.2; 2.25	sand; sst
				-30.1	-4.59	-10.43	0.0 ±0.2	84.3 ±2.0	5.3	28.05	150	75; 95	1.2; 2.25	sand; sst
				-30.4	-4.40	-10.49	0.0 ±0.2	66.0 ±1.8	20.3					
TT 163	H26-0470	5.7 ±1.3	64.0											Basalt 120m
TT 164	H26-0505	55.3 ±1.7	91.9											Basalt (Low y)
TT 165	H26-0510	58.3 ±1.8	57.1	-29.9	-4.77	-10.20	0.2 ±0.2	55.5 ±1.7	35.2					
TT 166	H26-0439	52.3 ±1.7	35.7			-12.66		54.7 ±1.7						Sst
						-12.76		48.8 ±1.7						Sst
				-32.5	-5.06	-14.17	0.2 ±0.2	71.5 ±1.9	24.1	36.8	340	60	7	bas; sst; sil; tuf
				-30.1	-4.76	-13.66	0.0 ±0.2	69.2 ±1.9	0.0	36.8	340	60	7	bas; sst; sil; tuf
				-31.1	-4.83	-13.77	0.0 ±0.2	71.8 ±1.9	45.3					
TT 167	H26-0484	87.9 ±2.0	3.8											Basalt (Low y)
TT 168	H26-0488	101.0 ±2.1	3.5	-28.7	-4.20	-9.07	0.5 ±0.2	112.8 ±2.2	99.1					Basalt
TT 169	H26-0487 (A)	0.0 ±1.2	70.6	-32.6	-5.56		0.1 ±0.2	0.0 ±1.2	137.1					Sst
TT 170	H26-0487 (B)	3.2 ±1.2												Sst
TT 171	H26-0516	89.2 ±2.0	138.7											Lineament
TT 172	H26-0443	92.3 ±2.0												Basalt
TT 173	H11-1743	84.9 ±2.0	3.9	-36.7	-6.35	-12.26	0.0 ±0.2	92.9 ±2.1	5.8	Deep	250	Dry		Qzte; bas
TT 174	H26-0457 (A)	22.8 ±1.5	1.3											Sst (Prod Bh)
TT 175	H26-0457 (B)	21.8 ±1.4		-32.4	-5.30	-12.94	0.0 ±0.2	53.8 ±1.8	3.3	49.2	237	118	40	bas; sst
				-32.6	-6.13	-15.03	0.0 ±0.2	23.5 ±1.5	21.4	49.2	237	118	40	bas; sst
				-31.5	-5.80	-15.26	0.0 ±0.2	25.7 ±1.5	0.0	49.2	237	118	40	bas; sst
TT 176	H26-0606 (A)	85.6 ±2.0	10.6											Sst (Prod Bh)
TT 177	H26-0606 (B)	82.1 ±1.9												Sst (Prod Bh)

2.2 General description of the Bochum study area

The Bochum settlements lie the north-western part of central Limpopo Province, located some 80km northwest of Polokwane and 25 km from Dendron.

The area lies to the south of the Blouberg Mountain. The lowest point is located in the north-western part area at approximately 900 m above sea level. Most villages are located in flat gently rolling terrain on the south, the western part being sparsely populated (Figures 1, 2)

The mean annual precipitation is 453 mm as recorded at Bochum rainfall station (0721/257). The two main drainages are the Brak River catchment and Mogalakwena River catchment in the west. Vegetation ranges from dense - short bushveld as well as open tree savanna to moist mountain bushveld in the lower-lying areas.

2.3 Regional and Structural Geology

The major part of the study area, which forms part of the southern zone of the Limpopo Mobile Belt, is underlain by medium to coarse grained, pinkish grey and pink leucocratic Houtrivier Gneiss, partly exposed in higher lying areas (Figure 1). Sedimentary rocks belonging to either the Waterberg or Soutpansberg Groups of rocks form the higher lying and mountainous areas to the north and west of the study area. These rocks include sandstone, conglomerate, grit, quartzite, arkose, mudstone, volcanic and volcano-clastic rocks (Geocon, 1997).

The Melinda fault forms the northern boundary of the shear zone and runs all the way into the study area in an east-north-easterly direction. The Melinda fault splits into a complex fault zone with numerous faults to be found both north and south. No major faults occur in the Houtrivier gneiss away from the mountain.

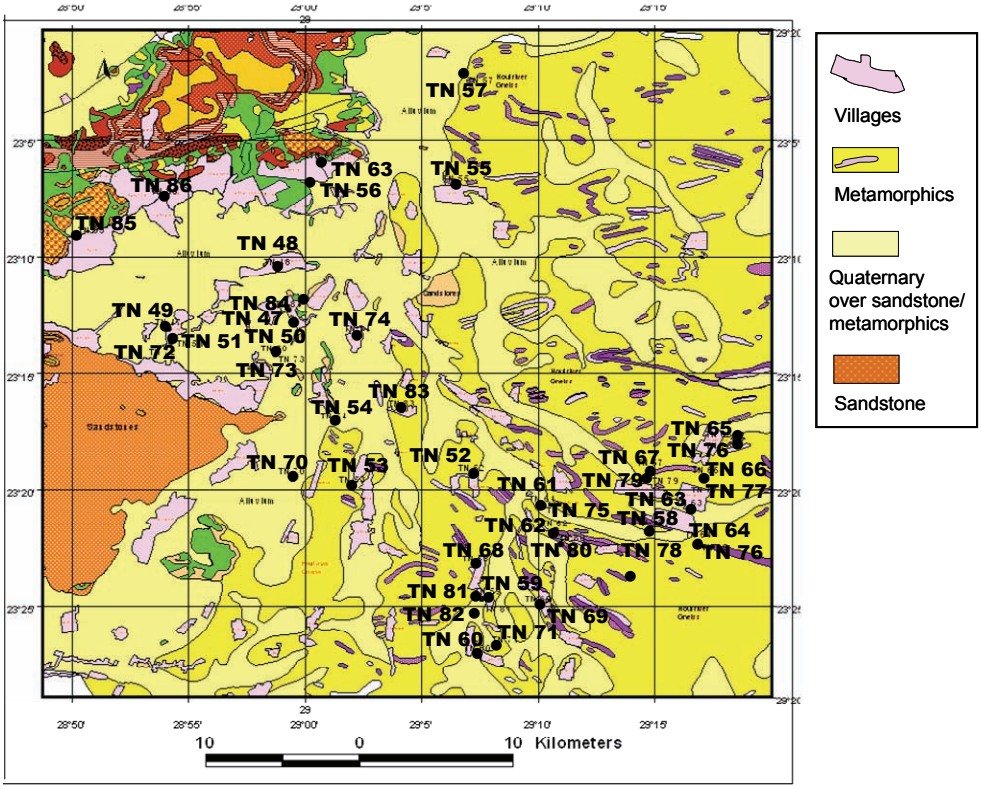

Figure 1; Geological map of the Bochum study area showing sampling points

2.4 Hydrogeology

Ground water potential varies dramatically throughout the study area and is determined mainly by the specific lithologies underlying each terrain. Increased ground water potential is found in sand and gravel deposits associated with the Brak River drainage with enhanced recharge potential towards the deeper lying fractured aquifers (Geocon, 1997).

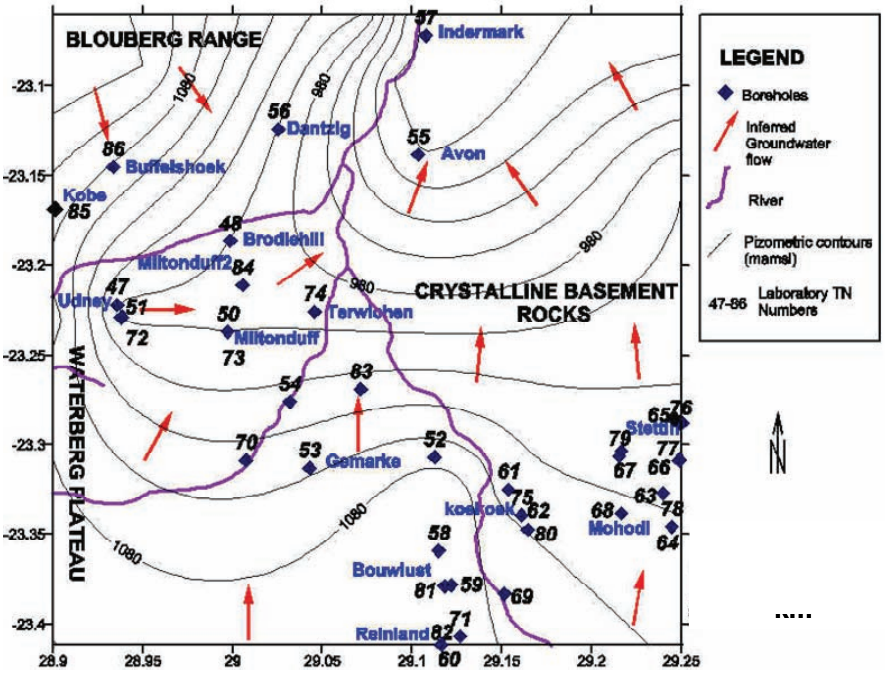

Figure 2: Map of the Bochum study area showing piezometric contours and inferred ground water flow directions

Only low ground water potential is associated with dolerite contact zones in the sedimentary rocks of the Waterberg and Soutpansberg Groups

The ground water potential in the metamorphic and associated rocks is generally determined by the grade of metamorphism. Rocks subjected to a higher grade of metamorphism typically display a resistance to weathering, fractures and ground water occurrences being less common. The depth to ground water is generally greater in the sandstones in the west than in the metamorphic rocks. This may be controlled by contrasting depth of fracturing and weathering in the two terrains and have a bearing on the pollution potential.

3. Methods

3.1 Field procedures

A set of samples was collected in April, 2005 and a smaller set in October 2007 that included some from several boreholes sampled previously in 2005. The sampling locations are shown on Figure 1.

Sample collection in the field followed as far as possible standard procedures (e.g. Clark and Fritz 1997; Weaver 1992) to ensure representativity of *in situ* water. Samples are taken straight from the outlet where wells, either motorised or hand-pumped, are in regular production at the time. Where the pump had been idle, the pump was operated until well-head observations on the water stabilised.

Large volumes of up to 100 litres of sample water are required for conventional radiocarbon analysis to harvest enough total dissolved inorganic carbon (TDIC) for analysis. The water is rendered alkaline (pH > 9) in a drum and the TDIC precipitated by adding $BaCl_2$. The usual well head observations are performed for temperature, EC, pH and TAlk (where pH >6). In some instances, Eh and dissolved oxygen are measured.

Several other observations were recorded at the well head, e.g. general location, well geographic co-ordinates, water temperature, pH, electrical conductivity, dissolved oxygen, TAlk. These have been recorded separately for the 2005 and 2007 samples in Tables 2a,b and 3a,b,c

Table 2a: Isotope and field data for Bochum study, March 2005.

Lab No.	Sample Identification	Latitude	Longitude	Date Sampled	E.C. (µS/cm)	Temp (°C)	pH	Alkalinity (meq/l)	Diss O_2 (mg/l)	Radon (CPMa)	δ D (‰)	$\delta^{18}O$ (‰)	Tritium (T.U.)	Carbon-14 (pMC)	$\delta^{13}C$ (‰)	$\delta^{15}N$ (‰)
TN 47	H11-1874	-23.22201	28.93562	15-Mar-05	2730	24.2	7.22	578.3	0.6	109.9	-23.0	-3.90	1.2 ±0.2	94.7 ±2.0	-7.20	+6.7
TN 48	H11-1196	-23.18677	28.99861	15-Mar-05	899	25.7	6.33	65.9	1.6	2521.6	-24.2	-4.31	1.7 ±0.2	96.1 ±2.0	-10.34	+9.5
TN 49	H11-1187			15-Mar-05	2390	26.3	6.80	248.9	0.5	411.2	-27.9	-4.69	1.9 ±0.2	102.1 ±2.1	-12.72	+11.7
TN 50	H11-1855	-23.23712	28.99725	15-Mar-05	5210	25.4	6.90	634.4	0.5	462.3	-28.3	-4.65	1.3 ±0.2	93.0 ±2.0	-7.14	+13.3
TN 51	H11-1208	-23.22861	28.93861	15-Mar-05	1636	25.8	7.20	524.6	0.7	704.6	-27.1	-4.53	1.3 ±0.2	104.7 ±2.1	-8.16	+8.4
TN 52	Overdyk1	-23.30695	29.11252	15-Mar-05	2450	26.8	7.47	378.2	0.3	71.2	-24.3	-3.91	1.4 ±0.2	104.0 ±2.1	-5.49	+5.6
TN 53	H11-1098	-23.31306	29.04278	15-Mar-05	1727	25.9	7.40	500.2	2.7	389.7	-29.1	-4.50	0.7 ±0.2	85.4 ±2.0	-5.76	+5.1
TN 54	H11-1162	-23.27615	29.03170	15-Mar-05	1195	24.8	7.57	624.6	-	72.2	-24.6	-4.16	1.1 ±0.2	94.5 ±2.0	-5.68	+5.6
TN 55	Avon1	-23.13839	29.10329	16-Mar-05	1649	24.4	7.41	592.9	3.5	17.2	-30.3	-4.62	0.5 ±0.2	97.7 ±2.1	-5.55	+6.0
TN 56	Dansig1	-23.12437	29.02552	16-Mar-05	413	24.9	7.31	258.6	0.9	745.5	-32.5	-6.18	0.1 ±0.2	83.7 ±2.0	-11.54	
TN 57	Indermark	-23.07189	29.10757	16-Mar-05	1292	26.0	7.46	556.3	5.2	28.9	-29.6	-5.10	4.5 ±0.2	94.8 ±2.0	-4.33	+2.2
TN 58	Boulust1	-23.35938	29.11477	16-Mar-05	1473	24.2	7.32	451.4	0.5	56.9	-28.6	-4.74	0.0 ±0.2	92.9 ±2.0	-6.55	+12.0
TN 59	Boulust2	-23.37827	29.12201	16-Mar-05	1757	25.9	7.35	446.5	0.9	230.3	-29.9	-4.79	0.3 ±0.2	87.3 ±2.0	-6.46	+8.8
TN 60	Rheinland	-23.40693	29.12661	16-Mar-05	1027	24.9	7.31	373.3	2.1	113.2	-29.7	-4.80	0.2 ±0.2	99.1 ±2.1	-6.57	+5.1
TN 61	Koekoek1	-23.32484	29.15374	16-Mar-05	1781	27.1	7.22	463.6	1.8	272.7	-27.1	-4.41	0.0 ±0.2	84.7 ±2.0	-6.38	+8.1
TN 62	Koekoek2	-23.33932	29.16084	16-Mar-05	1709	25.7	7.05	400.2	0.6	113.3	-25.1	-3.94	0.9 ±0.2	96.6 ±2.1	-6.41	+10.7
TN 63	H11-0805	-23.32692	29.23967	17-Mar-05	1781	24.1	7.35	388.0	6.1	181.0	-30.7	-4.59	0.7 ±0.2	100.8 ±2.1	-6.37	+0.3
TN 64	H11-1799	-23.34590	29.24459	17-Mar-05	1270	23.8	7.57	483.1	5.8	42.4	-35.3	-5.13	0.3 ±0.2	96.9 ±2.1	-6.20	-2.3
TN 65	H11-1330	-23.28667	29.26667	17-Mar-05	815	24.8	7.75	436.8	-	9.6	-21.1	-2.99	0.9 ±0.2	89.0 ±2.0	-5.40	
TN 66	H11-1335	-23.30811	29.24892	17-Mar-05	1071	26.2	7.84	480.7	5.3	31.0	-31.2	-4.91	0.0 ±0.2	81.9 ±1.9	-7.03	
TN 67	H11-0002	-23.30345	29.21642	17-Mar-05	1070	24.9	7.91	473.4	-	20.3	-32.2	-4.93	0.0 ±0.2	86.9 ±2.0	-5.80	
TN 68	Schellenburg	-23.33821	29.21646	17-Mar-05	1711	24.7	7.51	366.0	2.0	113.6	-26.5	-4.26	1.3 ±0.2	107.1 ±2.1	-5.91	-3.5
TN 69	H11-1465	-23.38317	29.15143	17-Mar-05	1326	24.8	7.50	568.5	0.5	42.9	-33.7	-5.01	0.0 ±0.2	93.1 ±2.0	-7.10	+8.0
TN 70	Skoonveld	-23.30872	29.00734	17-Mar-05	829	25.0	8.05	258.6	0.2	16.7	-25.5	-3.78	0.4 ±0.2	95.5 ±2.0	-5.74	
TN 71	H11-0698	-23.41144	29.11610	17-Mar-05	1252	25.6	7.54	446.5	5.7?	281.0	-30.3	-4.45	0.3 ±0.2	87.5 ±2.0	-4.84	-1.0

Table 2b: Geology, pump and major ion data for Bochum study, March 2005.

Lab No.	Geology	Pump	Comments	pH	NO3-N (mg/l	F (mg/l)	TAL (mg/l)	Na (mg/l)	Mg (mg/l)	Si (mg/l)	SO4 (mg/l)	Cl (mg/l)	K (mg/l)	Ca (mg/l)
TN 47	Sandstone	Handpump		7.94	14.3	0.80	447.0	385.2	68.0	36.0	56.7	559.4	1.3	117.3
TN 48	Sandstone	Handpump	In school yard	7.35	39.0	0.20	40.8	45.8	31.9	20.4	27.4	136.4	17.9	58.8
TN 49	Sandstone	Handpump												
TN 50	Sandstone	Handpump		7.63	52.0	0.31	462.0	604.2	195.5	27.5	98.6	1316.5	13.1	171.2
TN 51	Sandstone	Handpump		7.65	14.2	0.55	401.0	183.1	47.0	34.2	18.3	268.3	1.9	101.0
TN 52	Granite	Handpump		7.73	3.4	0.58	318.4	264.1	96.2	38.9	110.6	291.6	19.4	106.4
TN 53	Granite	Handpump	Recent bad smell	8.04	156.5	0.43	393.1	176.9	73.7	35.3	38.6	267.2	18.2	78.6
TN 54	Granite	Handpump	Cattle drinking, standing wat	8.00	121.3	0.77	499.0	126.6	67.6	39.3	21.3	95.9	16.3	43.2
TN 55	Granite	Handpump		7.94	20.2	0.26	487.0	105.8	120.3	29.8	58.0	202.0	12.7	76.5
TN 56	Granite/Sst	Handpump		8.16	0.5	0.20	190.4	17.8	20.4	26.1	6.8	12.3	0.9	38.6
TN 57	Granite	Handpump	5m from cattle enclosure	8.02	9.3	0.27	441.0	86.0	95.4	39.2	38.4	147.0	8.4	58.6
TN 58	Granite	Handpump	Alongside maize field	7.83	25.5	0.33	365.3	167.1	56.2	37.8	32.4	198.0	24.5	62.1
TN 59	Granite	Handpump	Casing to 24m	7.67	52.4	0.40	365.9	176.5	81.7	36.1	48.2	231.4	19.4	87.1
TN 60	Granite	Handpump	In school	7.52	8.0	0.44	305.2	147.5	37.1	39.8	20.9	143.5	4.3	32.6
TN 61	Granite	Handpump	Alongside sheep enclosure	7.99	20.3	0.21	360.3	191.6	70.1	37.5	45.0	306.2	11.7	88.4
TN 62	Granite	Handpump		7.55	41.5	0.29	306.9	177.3	88.4	39.7	68.8	259.3	12.8	59.3
TN 63	Granite	Borehole		7.84	20.3	0.25	305.0	143.3	91.7	36.1	55.9	336.9	9.2	91.7
TN 64	Granite	Borehole		8.02	9.5	0.29	362.7	120.2	61.4	38.6	40.7	174.6	13.9	63.2
TN 65	Granite	Borehole		8.17	<0.08	0.21	353.1	71.9	50.9	39.3	14.9	52.3	9.4	31.0
TN 66	Granite	Borehole		7.72	2.0	0.21	390.2	113.7	56.1	39.7	24.2	123.6	12.2	48.4
TN 67	Granite	Borehole		7.79	5.1	0.18	363.1	89.3	67.9	39.6	25.9	122.6	11.8	39.0
TN 68	Granite	Handpump	Cattle enclosure 25m away	7.88	63.9	0.44	274.0	164.1	77.6	38.8	67.2	202.0	16.4	78.5
TN 69	Granite	Handpump		7.94	55.9	0.42	447.0	144.3	61.0	34.0	28.4	156.1	14.0	57.6
TN 70	Granite	Handpump	Water black	8.27	0.7	0.21	178.5	112.0	19.4	2.2	8.4	152.9	11.3	21.6
TN 71	Granite	Borehole		7.93	12.4	0.37	340.6	143.9	47.5	30.9	39.9	155.3	11.5	59.6

Table 3a: Isotope and sample data for Bochum study, October 2007.

Laboratory Number	Sample Identification	δ D (‰)	$\delta^{18}O$ (‰)	Tritium (T.U.)	Carbon-14 (pMC)	$\delta^{13}C$ (‰)
TN 72	H11-1848 Milbank 02/10/2007	-33.6	-4.80	0.5 ±0.2	93.0 ±2.0	-8.41
TN 73	H11-1855 Miltonduff 02/10/2007	-30.1	-4.46	0.8 ±0.2	94.7 ±2.0	-7.37
TN 74	H11-1176 Terwichen/Ga-Rammutla 02/10/2007	-33.6	-4.73	0.7 ±0.2	96.2 ±2.0	-5.90
TN 75	H11-0052 Koekoek 1 02/10/2007					
TN 76	H11-0876 Stettin 1/Ga-Madikana 03/10/2007	-22.5	-2.94	1.5 ±0.3		
TN 77	H11-1335 Stettin 2/Ga-Madikana 03/10/2007	-34.4	-4.84	0.4 ±0.2	88.8 ±2.0	-7.32
TN 78	H11-1799 Mohodi 03/10/2007	-37.4	-5.28	0.8 ±0.2	105.8 ±2.1	-5.91
TN 79	H11-1698 Koningkratz/Ga-Maponto 03/10/2007	-34.4	-4.91	0.0 ±0.2	86.9 ±2.0	-7.19
TN 80	H11-0818 Koekoek 2 03/10/2007	-30.6	-4.46	0.9 ±0.2	89.4 ±2.0	-5.05
TN 81	H11-1672 Boulust 03/10/2007	-32.9	-4.75	0.3 ±0.2	85.1 ±2.0	-6.32
TN 82	H11-0698 Rheinland 03/10/2007	-31.7	-4.69	1.5 ±0.2	89.4 ±2.0	-6.01
TN 83	H11-1166 Witten-B 04/10/2007	-32.6	-4.78	0.4 ±0.2	87.9 ±2.0	-4.74
TN 84	Miltonduff 04/10/2007	-28.1	-4.53	2.4 ±0.3	108.9 ±2.1	-13.60
TN 85	H11-1915 Blackhill/Ga-Kobe 04/10/2007	-33.4	-5.53	1.9 ±0.3	109.8 ±2.1	-16.42
TN 86	H11-0505 Buffelshoek 04/10/2007	-34.9	-5.66	1.0 ±0.2	99.2 ±2.1	-6.98

Table 3b: Major ion analyses for Bochum study, October 2007.

Laboratory Number	Ca mg/l	Mg mg/l	Na mg/l	K mg/l	Si mg/l	HCO3 mg/l	SO4 mg/l	Cl mg/l	NO3 mg/l	F mg/l
TN 72	173	107	393	0.97	36.3	563.6	48.3	799.7	63	0.4
TN 73	210	214	868	11.2	32.2	556.3	125.3	1541.2	565.5	0.1
TN 74	135	251	793	9.72	40.3	571.0	203.8	1762.5	44.3	0.0
TN 75	115	88.3	200	15	37.4	537.0	48.8	435.1	0.0	0.1
TN 76	31.4	52.7	75.1	9.4	42.4	507.5	16.7	60.9	13.5	0.1
TN 77	51.6	58.4	103	11.9	41.3	356.2	28.3	126.9	11.6	0.1
TN 78	64	62.1	119	13.4	40.2	319.6	42.5	168.6	37.4	0.2
TN 79	35.6	65.4	77	9.33	40.1	385.5	21.3	108.1	10.0	0.1
TN 80	49.6	42.7	160	12	35	456.3	20.2	118.7	53.1	0.3
TN 81	58.1	52	127	15.2	34.5	370.9	34.1	159.6	38.8	0.3
TN 82	66.5	48.4	140	11	32.7	482.0	47.0	147.8	75.0	0.2
TN 83	62.9	65.3	183	14.8	40	588.0	103	205.8	37.3	0.3
TN 84	7.7	7.0	27.8	31.8	41.9	83.0	12.8	54.9	12.3	0.1
TN 85	5.1	5.01	9.61	1.12	7.42	14.2	0.7	22.8	18.2	0.0
TN 86	47.2	41.5	28.2	0.37	24.1	344.0	5.8	49.7	13.2	0.2

Table 3c; Field observations for Bochum study, October 2007.

TN No.	Sampling Date	Borehole Number	Farm/Village Name	Longitude	Latitude	Altitude mamsl	pH	EC µS/cm	Temp oC	Diss Oxygen	General Comments
72	02/10/2007	H11-1848	Milbank	23.22908	28.93769	967	6.87	3600	23.8	3.61	handpump Monyabodi School Domestic taste strangely sweet
73	02/10/2007	H11-1855	Miltonduff	23.23712	28.99725	993	6.86	6870	24.7	3.11	hand pump in settlemet cattle drinking trough taste saline/sweet
74	02/10/2007	H11-1176	Terwichen/Ga-Rammutl	23.22583	29.04569	925	7.01	6481	25.8	3.45	hand pump houses @50m cattle drinking trough tastesaline sweetish
75	02/10/2007	H11-0052	Koekoek 1	23.32484	29.15374	1013	N/M	N/M	N/M	N/M	handpump polluted (latrine) gardening use previously sampled
76	03/10/2007	H11-0876	Stettin 1/Ga-Madikana	23.28482	29.26668	1024	7.99	879	24.4	8.20	production bh outskirts of settlement, on rise quartz pebbles taste perfect
77	03/10/2007	H11-1335	Stettin 2/Ga-Madikana	23.30880	29.24869	1036	7.71	1168	24.3	7.05	production bh far from settlement deforested, sandy stunted trees taste good
78	03/10/2007	H11-1799	Mohodi	23.34590	29.24459	1026	7.70	1371	24.7	7.11	production bh outskirts of settlement, surrounded by vegetation
79	03/10/2007	H11-1698	Koningkratz/Ga-Mapont	23.30645	29.21542	1003	7.65	1040	25.2	6.03	production bh, outskirts of settlement, deforested sloping terrain, spillage
80	03/10/2007	H11-0818	Koekoek 2	23.34743	29.16436	1009	7.88	1310	25.4	5.18	production bh, settlement @ 150m, deforested, small-scale irrigation
81	03/10/2007	H11-1672	Boulust	23.37894	29.11798	1034	7.58	1302	25.2	2.36	productionbh, settlement @ 100m small cemetery @ 50m coarse sand, thorn bush
82	03/10/2007	H11-0698	Rheinland	23.41223	29.11601	1073	7.35	1952	35.4	1.96	production bh, settlement @ 50m upslope, coarse, claey sand, bush
83	04/10/2007	H11-1166	Witten-B	23.26904	29.07143	972	7.36	1654	25.3	5.01	production bh, edge of settlement, deforested, sloping, coarse sand
84	04/10/2007	No number	Miltonduff	23.21126	29.00547	932	6.60	340	25.7	5.53	hand pump in settlement, little used, s/s outcrops sloping terrain close to tarred road
85	04/10/2007	H11-1915	Blackhill/Ga-Kobe	23.16807	28.88263	1033	5.46	133	25.6	N/M	hand pump at foot of Blouberg supplies big population erosion and overgrazing, aloes
86	04/10/2007	H11- 0505	Buffelshoek	23.14520	28.93339	987	7.22	664	27.0	N/M	production bh, flat flood plain(?) surrounded by settlement, deforested nearby river/erosion

3.2 Analytical procedures

Analyses for environmental isotope values were conducted by the Environmental Isotope Laboratory of iThemba LABS (Gauteng). Parameters measured in the 2005 samples were: δ^2H, $\delta^{18}O$, $\delta^{13}C$, $\delta^{15}N$, ^3H, ^{14}C and ^{222}Rn. No samples for ^{222}Rn were taken in 2007. Due to analytical problems, no $\delta^{15}N$ analyses were conducted on the 2007 samples.

Major ion concentrations were conducted by standard on-line procedures. The 2005 samples were analysed by the DWAF laboratories; the 2007 samples by a commercial laboratory. The results for the two sampling periods are presented in Tables 2 and 3.

3.3 Environmental isotope analysis.

Isotopic analyses were performed by the Environmental Isotope Laboratory of iThemba LABS (Gauteng).

$^{18}O/^{16}O$ ratios were analysed by equilibrating a small aliquot of water with CO_2 gas, which is then introduced into an isotope-ratio mass-spectrometer (IRMS). In $^2H/^1H$ analysis, water is

equilibrated with H_2 gas in the presence of a platinum catalyst. Isotope ratios are expressed as relative differences $\delta = \{(R_s-R_r)/R_s\}*1000$ ‰ w.r.t. a reference standard, where R_s and R_r represent isotope ratios of the sample and reference standard, respectively. These are then normalised as δ^2H and $\delta^{18}O$ in ‰ with respect to the international VSMOW scale. Analytical precision is usually better than 0.1 ‰ for $\delta^{18}O$ and 0.5‰ for δ^2H.

Stable carbon isotope ratios ($^{13}C/^{12}C$) are determined on CO_2 gas by acidification of either the field precipitate or by direct acidification of the water sample. They are expressed as $\delta^{13}C$ in ‰ with respect to the international VPDB standard with typical 1σ errors better than ±0.2‰.

Stable nitrogen isotope ratios ($^{15}N/^{14}N$) in nitrate are determined by reducing the total dissolved inorganic nitrogen to NH_3 which is reacted with H_2SO_4.The resulting NH_4SO_4 is then pyrolised on line and reduced to N_2 gas which is introduced into an IRMS. The results are expressed as $\delta^{15}N$ in ‰ w.r.t. atmospheric N_2. The intrinsic accuracy of the method is rather low, with typical errors of the order of 0.3 to 0.5 ‰.

Radiocarbon was measured by evolving CO_2 from the field precipitate which is absorbed in an organic scintillation cocktail that is introduced into an ultra-low level liquid scintillation spectrometer. Results are normalised to an NBS and IAEA standard and expressed in pMC (per cent modern carbon). Typical 1σ errors are better than ±0.5 pMC and ±2 pMC respectively. Present-day radiocarbon values in atmospheric CO_2 are about 110 pMC.

In tritium (^3H) analysis, the water sample is first electrolytically pre-enriched by a factor of 20, the distilled product water mixed with an organic scintillation cocktail and measured in an ultra low-level liquid scintillation spectrometer. The results are expressed as tritium units (TU $\equiv {}^3H/{}^1H = 10^{-18}$) normalised to an NBS and IAEA standard. The 1σ precision (in the range up to ~ 5 TU) is ±0.2 TU. Present-day rainfall tritium values are in the range of 3-5 TU in southern Africa (GNIP - http://isohis.iaea.org).

3.4 Calculation of ^{14}C mean residence time, or age

Under phreatic aquifer conditions, the isotope-based mean residence time (MRT in years) of ground water was calculated (Verhagen et al. 1991) from the ^{14}C content using

$$MRT = 8267*\{(A_0/A) -1\}$$

where A is the analyzed ^{14}C activity of the sample and an appropriate value of the initial ^{14}C activity A_0.

The vegetation in the area of study consists of a mixture of C3 and C4 plants, resulting in a probable range of values of $\delta^{13}C$ for soil CO_2 of ~ -23 ‰ to -14 ‰. Corrections for isotopic exchange and fractionation factors for ^{14}C on the basis of observed $\delta^{13}C$ values of TDIC may be applied according to various proposed models (Clark & Fritz 1997). Such corrections may introduce even larger errors (Verhagen et al. 1991). Assuming an initial (recharge) value of 80% to 90% of atmospheric CO_2 is often a safe value of A_o to adopt.

3.5 Exponential model plot

Plotting radiocarbon against tritium data may be employed to assess aquifer behaviour as well as assess mean residence time. Such plots can be fitted with curves of the known isotope input function (e.g. records of tritium in rain and radiocarbon in atmospheric CO_2) based on

different models of aquifer behaviour. The response of an ideal phreatic aquifer may be approximated by the convolution integral expressing well-mixed model (Verhagen et al. 1991)

$$A(t) = \int_0^\infty A_0(t-\tau) e^{-\lambda t} f(\tau) d\tau$$

In this equation, A(t) is the observed tracer concentration at time t; $A_o(t-\tau)$ is the (known) input concentration as a function of time t and the transit time τ; λ the decay constant of the relevant isotope and $f(\tau)$ is the aquifer response function, which for the exponential model is:

$$f(\tau) = \frac{e^{-\tau/T}}{T}$$

where T is the mean ground water residence time.

Reverse modelling determines the expected tracer concentration of an ideal, uniformly recharged aquifer as a function of mean residence time.

4. Discussion of the analytical data

4.1 Radiocarbon corrections

In certain environments, ground water hydrochemical processes involving TDIC (total dissolved inorganic carbon) may alter the radiocarbon concentration. These may be adjusted according to the changes in $\delta^{13}C$. Such processes often become evident in a correlation between $\delta^{13}C$ and ^{14}C, where older water (lower ^{14}C) shows an increase in $\delta^{13}C$, evidence of ongoing isotope exchange or dilution processes with aquifer material.

Figure 3 shows a plot of $\delta^{13}C$ against ^{14}C for ground water in the Bochum area for both the 2005 and 2007 sample series. The main cluster of points, centered on ^{14}C ~ 95 pMC; $\delta^{13}C$ ~ -6 ‰ shows no clear trends for either data set. Only two samples taken from the sandstone

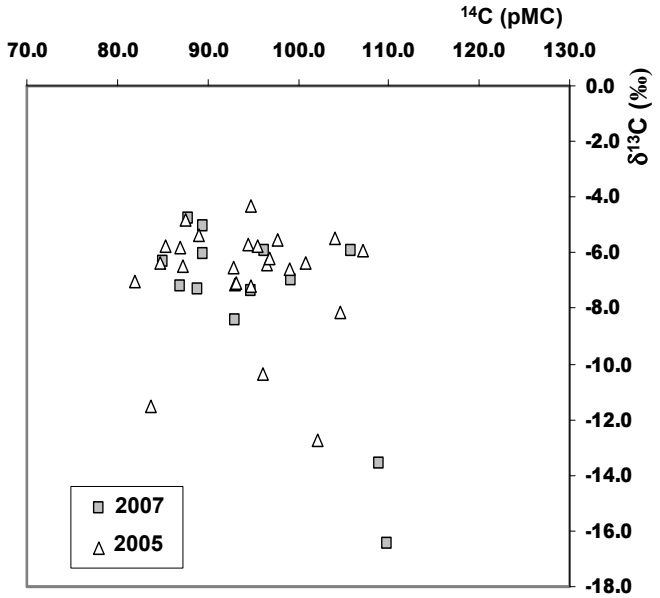

Figure 3: Scatter-plot of $\delta^{13}C$ against ^{14}C for the two sampling periods.

aquifer on the slopes of the Blouberg, with high ^{14}C and ^{3}H and low TAlk, EC and pH, show the low $\delta^{13}C$ values that characterise e.g. Table Mountain Sandstone water (Verhagen et al. 2008). The samples that fall in the cluster are chemically mature, the "youngest" of which have ^{14}C values that trend only marginally below those of the mountain slope samples.

This suggests that there has been no major dilution of ^{14}C which reflects relative ages or residence times. This is in accord with both the geology of the area as well as observed soil conditions that are essentially free of limestones and secondary carbonate deposits (calcretes).

4.2 Radiocarbon and tritium

Radiocarbon values are plotted against tritium values for both 2005 and 2007 samples in Figure 4. Whereas tritium values range from 0 TU up to 4.6 TU, the range of ^{14}C values is relatively narrow, from 80 pMC to 107 pMC. Superimposed on the scattergram are the exponential model plots (see above; Verhagen et al. 1991) of ^{14}C against ^{3}H values with initial, or recharge, ^{14}C concentration A_o of 90% atmospheric that gave the best fit for the Taaibosch data, and of 80%.

The general trend of the plotted data conforms to the idealised model., There is a (small) category of points that lies well above the model plot $^{14}C \geq 100$ pMC; $^{3}H \leq 0.5$ TU as in the Taaibosch area; which could be ascribed to phreatophyte root transport of ^{14}C (Verhagen 2004a,b).

Where the results differ radically from those for Taaibosch is that the characteristically lower values of ^{14}C (< 80pMC) are missing for ^{3}H values trending towards 0 TU, as are mixed values ^{14}C < 80pMC and ^{3}H > 0.5 TU i.e. well below the curve. This suggests a completely different hydrology of fairly shallow circulating, recent ground water, in both the sandstones and the crystalline rocks. Especially in the latter, the (fracture) porosity may be expected to decline rapidly with increasing depth below surface. The ^{14}C values as shown in Figure 4 can

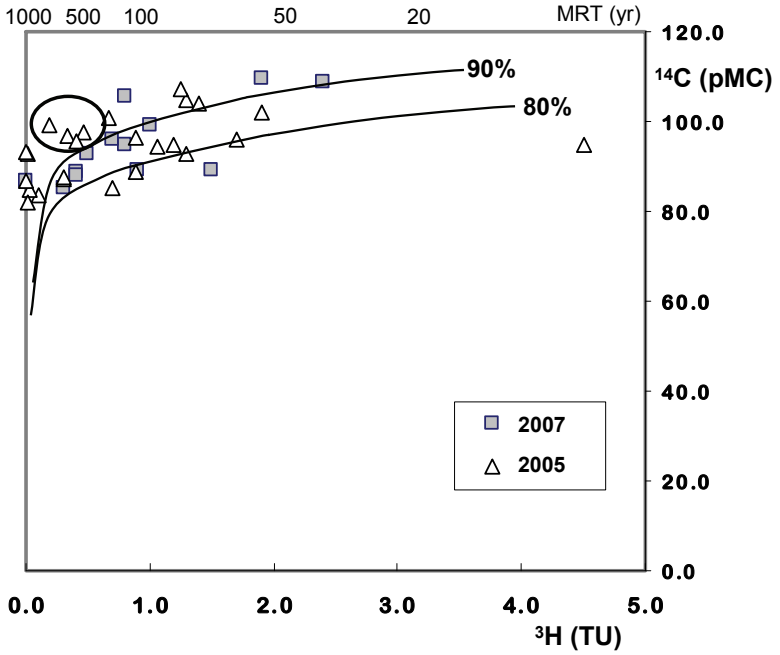

Figure 4: Scatter-plot of ^{14}C against ^{3}H for both sampling periods. Also shown are plots of expected exponential model values for different initial ^{14}C values and mean residence time, as shown along the top of the diagram

be interpreted (Sections 3.4; 3.5) as ground water mean residence times ranging from a few decades op to about 1000 years, implying fairly rapidly turned-over ground water. As the soil cover in the area is generally thin, both the aquifer groups should be vulnerable to surface pollutants. In the absence of details on probable aquifer porosities or borehole depths, isotope-based recharge rates cannot as yet be determined.

4.3 Stable isotopes – δ^2H and $\delta^{18}O$

Figure 5 shows a plot of δ^2H against $\delta^{18}O$ for the combined sampling periods with the global meteoric water line (GMWL; Clark and Fritz 1997) as reference. The values form a cluster around δ^2H ~ -27 ‰ and $\delta^{18}O$ ~ -4.7 ‰, very similar to observations for the Taaibosch area. As at Taaibosch, the linear regression line for the cluster has a slope of ~5, suggesting evaporative losses of rainwater before infiltration (Figure 5). Closer inspection however, shows that the low slope of the regression line is influenced strongly by a few outlier points at either end of the cluster. The larger body of points seems to be contained between the GMWL and a parallel line with a δ^2H intercept of ~ +5 ‰. This may reflect a local rainfall regime characterised by a local meteoric water line (LMWL), as was inferred for the Taaibosch area, where rainfall isotopic data was available for several years.

The Bochum stable isotope data therefore does not clearly reflect significant surface evaporative losses due to ponding of rain water. The study area is characterised by a rather flat topography, slightly undulating over the weathered granite with a marked drop in altitude to more level sandstone terrain to the west. The spread of data points does not suggest any particular difference in rainfall selectivity between the two main geological/physiographic terrains.

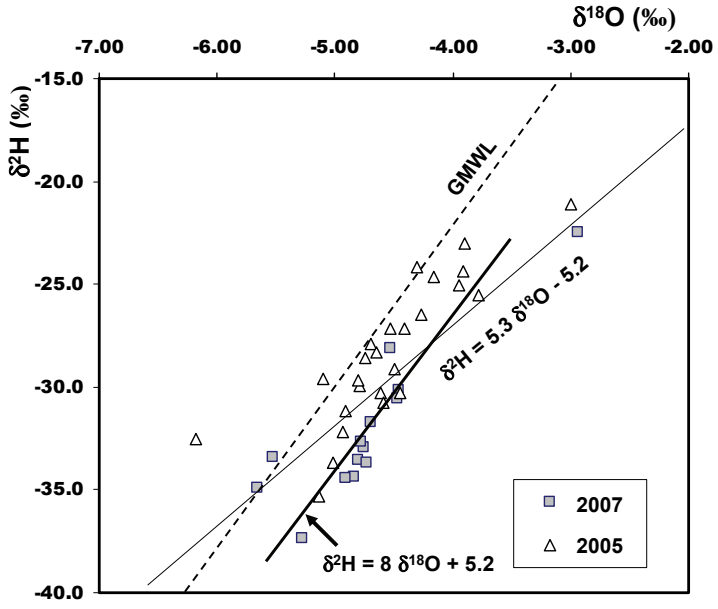

Figure 5: Scatter-plot of δ^2H against $\delta^{18}O$ for the two sampling periods, with a least mean squares fit to the points, the GMWL and a possible local meteoric water line (LMWL).

4.4 Major ion chemistry

The major ion chemistry for Bochum ground water is presented in Table 2b for samples taken in 2005 and Table 3b for 2007. Hydrochemical plots are presented in Figures 6 and 7.

With few exceptions, the overall mineralisation of the ground water samples is in the potable range. Samples with NO_3 concentrations above the potable limit of NO_3-N ≥ 10 mg/l account for some 60%, a percentage very similar to that found at Taaibosch. The majority of the samples for both 2005 and 2007 (Figures 6 and 7) cluster in the centre of the Piper diamond field, with a developmental trend of a gradual mineralisation in especially Na^+ and Cl^-, but also in Ca^{2+}, Mg^{2+}, HCO_3.

There is no evidence of significant ion exchange, as no points fall in the Na;HCO_3 sector of the Piper diagram, and the ratio of Ca/Na is rather constant. This is suggested too by a rather constant $\delta^{13}C/^{14}C$ relationship, with only few exceptions. The clustering seen in both Piper and Schoeller diagrams is very similar for the 2005 and 2007 sample sets.

An interesting feature of especially the Schoeller diagrams is the great similarity of the plots for all samples from the metamorphic granite, both in ionic ratios and in concentrations. A much greater spread is seen in the sandstone samples, where the most noticeable feature is the differences in Na and Cl. This suggests that the chemistry in the sandstone is determined more by extraneous influences, whilst in the granite the development is indigenous to the aquifer, determined by the abundant feldspars.

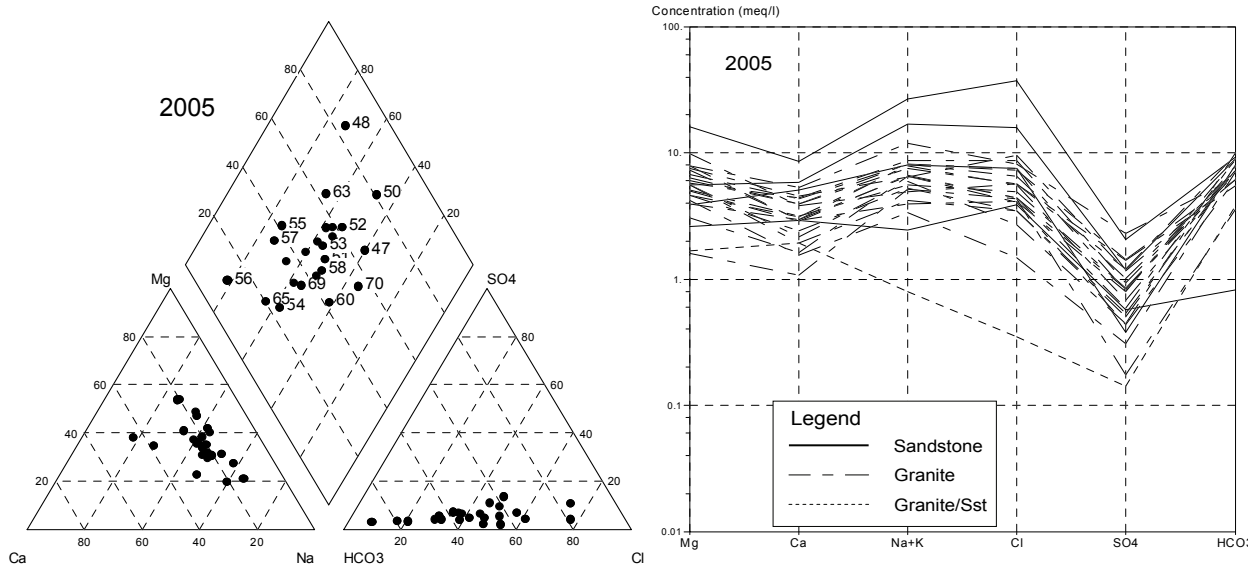

(a) (b)

Figure 6: Major ion chemistry for 2005 samples displayed on (a) a Piper and (b) a Schoeller diagram.

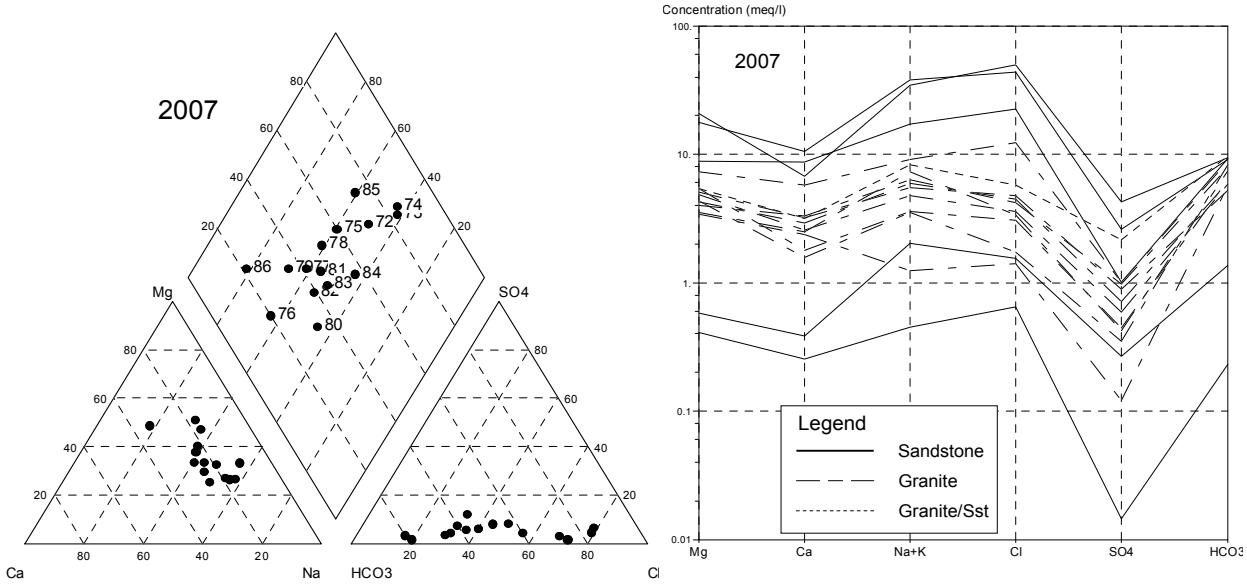

(a) (b)

Figure 7: Major ion chemistry for 2007 samples displayed on (a) a Piper and (b) a Schoeller diagram.

A Piper diagram for all the sample points coded for the different lithologies is displayed in Figure. 8. This shows clearly the development of the granite ground water from Ca,Mg-HCO_3 dominance to more mineralised types, albeit within a relatively narrow range of mineralisation. The sandstone samples plot quite separately, especially the more highly mineralised cases, whilst the few mixed cases tend to have quite different signatures.

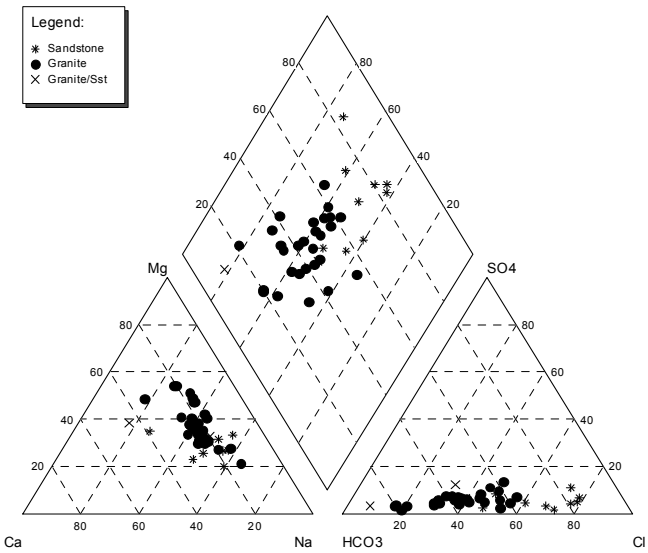

Figure 8: Piper diagram of combined major ion data for 2005 and 2007, grouped into three hydrogeological categories.

4.5 Nitrate development

The most prominent hydrochemical feature observed in Table 3 is the high proportion (63%) of samples with nitrate concentrations exceeding the generally accepted potable limit (WHO 1995) of 45 mg/l for NO_3^- or 10 mg/l for NO_3-N (Verhagen et al. 2004a), as well as some

exceedingly high values >100 mg/l. This percentage is similar to that found in the Taaibosch area. Especially in a densely populated rural village area such as Bochum, such figures tend to be associated with anthropogenic sources, such as sewage, cattle concentrations etc. Nitrate values do not appear to be influenced by either the aquifer environment, or the overall hydrochemical development.

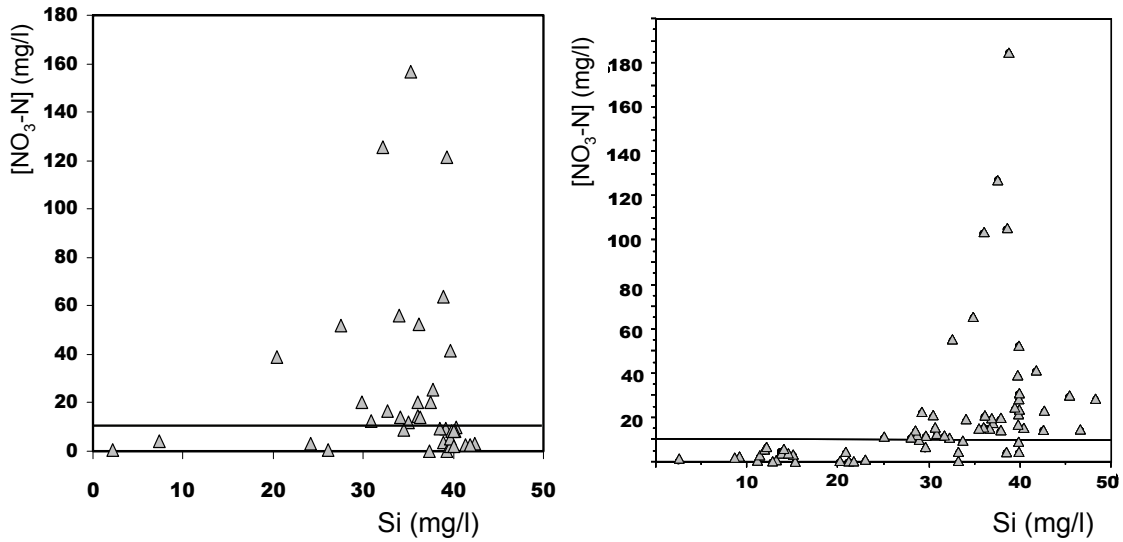

Figure 9: (a) Scatter plot of Si concentration against nitrate concentration for Bochum (b) scatter plot of NO_3 against Si for Phase I (Taaibosch).

An unexpected and striking feature of the data set from the Phase I (Taaibosch) study (Verhagen et al. 2004a,b) was that the only hydrochemical correlation that could be found with nitrate was with dissolved $Si(OH)_4$ (expressed as Si (mg/ℓ); see Figure 9(b)). This provided an important clue to the model of natural development of high(er) NO_3 concentrations in ground water. The decay of functional root material mobilises reduced nitrogen that is subsequently mineralised under oxic conditions, with the concomitant production of CO_2. The resulting drop in pH produces feldspar dissolution and mobilises Si. One of the motivations for this, Phase II of the study, was to establish whether similar processes would/could operate in another geological environment.

The comparative plot for Bochum in Figure 9(a) shows a similar trend of higher NO_3 values associated with the Si concentration range of 30-40 mg/ℓ, suggesting a similar mechanism of NO_3 production. It should be noticed that, in spite of the larger number of data points for Taaibosch, the number of high nitrate cases is similar for the two areas. This could be interpreted as the influence of upwelling, deeper sandstone, water into the basalt aquifer of Taaibosch, from which most of the samples were taken.

4.6 The relationship between NO_3 and residence time

Generally, the concentration of tritium in groundwater is an indication of the extent of local recharge, or recharge/storage ratio. The inverse of this relationship is a measure of mean residence time. Radiocarbon gives the same type of information, but on a longer time scale. Figure 10 shows the relationship between the concentration of NO_3 and respectively ^3H and ^{14}C.

For both the longer (^{14}C) and shorter (^3H) time scales, there is a trend of nitrate concentrations increase with increasing groundwater residence time. This trend may be seen as a build-up nitrate with increasing storage and/or depth. There is no discernible dependence of nitrate on

overall ground water mineralisation, expressed as EC. The primary natural source of ground water nitrate is taken to be the soil (Heaton 1984). In areas of thicker soil cover, the recharge rate would be lower due to evapotranspirative losses, with a concomitant increase in chloride. It is possible that at least part of the build-up with time is the result of the production of *nitrate at depth*. This conclusion is supported by the observed the increase of Si with NO_3, characteristic of Taaibosch ground water. (Section 4.5).

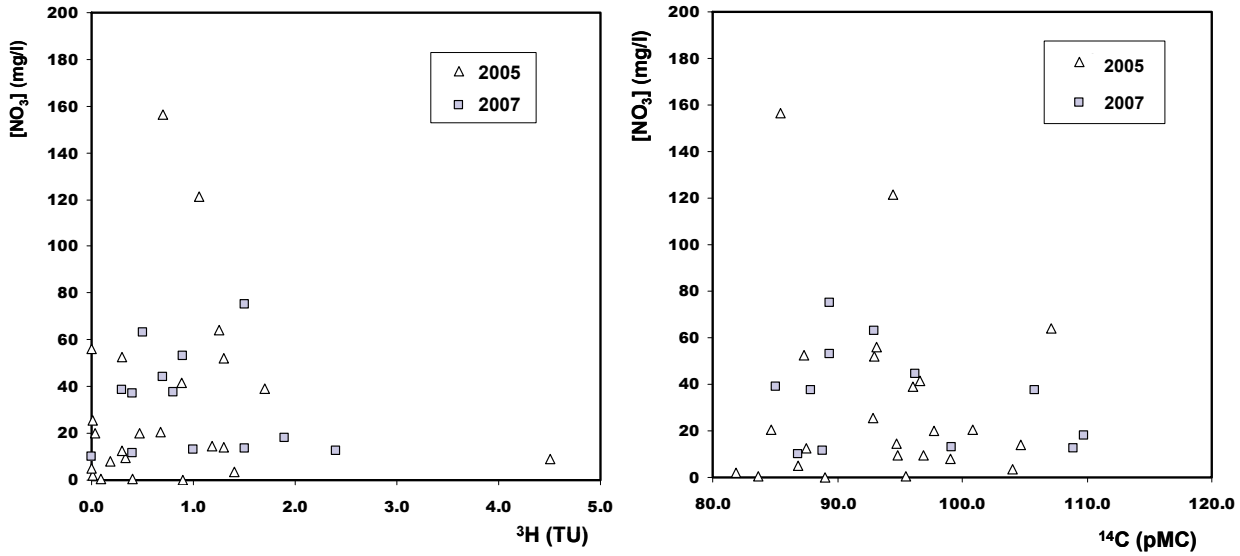

(a) (b)

Figure 10: Nitrate concentrations as a function of (a) tritium and (b) radiocarbon values.

4.7 Nitrogen-15 as a function of nitrate concentration

The value of $\delta^{15}N_{NO3}$ may act as an indicator of the source of nitrate in ground water (Heaton 1984). Values $\delta^{15}N < 10$ ‰ are generally taken as indicating natural sources as well as nitrate derived from artificial fertilisers. Values > +10 ‰, especially with attendant high nitrate concentrations, may indicate nitrate derived from animal and human waste.

Figure 11 shows no clear relationship between nitrate $\delta^{15}N$ and nitrate concentration in Bochum ground water. Most of the points fall below the potable limit of 45 mg/l. This group contains a wide range $\delta^{15}N$ values, ranging from -3 ‰ to a high of +12 ‰ which can be regarded as sewage associated. On the other hand, the higher nitrate concentration group shows "natural" $\delta^{15}N$ values.

High nitrate concentrations therefore appear to be generated not only by sources such as pit latrines, septic tanks or livestock concentrations in areas of active recharge or near boreholes with leaky collars. Nitrate input from tillage as well as the natural process such as identified in the Taaibosch study could also contribute. This relationship will have to be investigated in terms of a more thorough consideration of the location of individual boreholes. These remarks are to be read, however, in relation to the phenomenon of dentrification, that is discussed below.

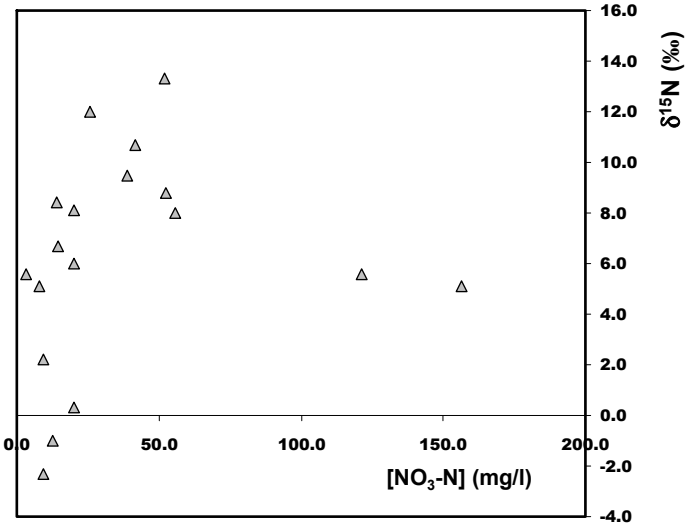

Figure 11: Ground water 2005 nitrate $\delta^{15}N$ values plotted against nitrate concentrations.

4.8 Denitrification

High $\delta^{15}N$ values are generated in the process of nitrate isotope fractionation during anaerobic fermentation of nitrogen-containing organic materials, e.g. proteins and nucleic acids. The separation of a volatile component (NH_3) that is highly depleted in the heavy ^{15}N isotope leaves the solid/dissolved residue correspondingly enriched (Clark and Fritz 1997). Subsequent mineralisation under oxic conditions generates nitrate with this high $\delta^{15}N$ signature. Where conditions subsequently introduce more dissolved organic material into ground water and dissolved oxygen values drop, nitrate in its turn is subjected to anaerobic bacterial breakdown, i.e. denitrification, $\delta^{15}N$ values of the remaining nitrate will increase.

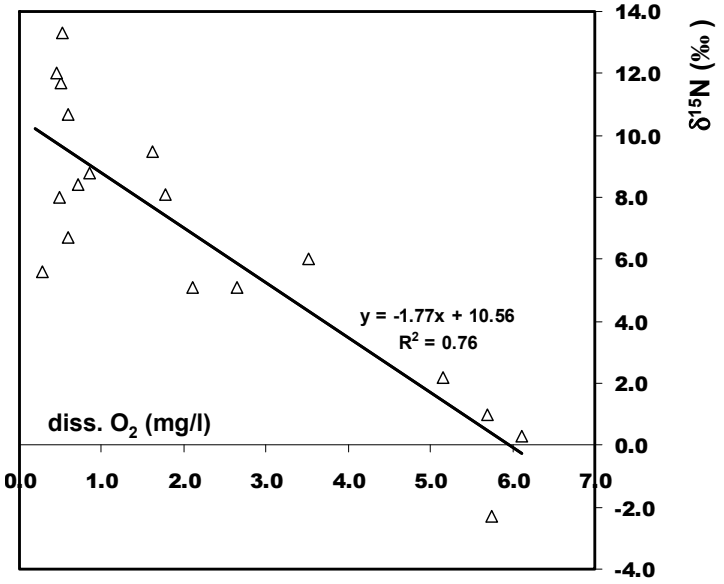

Figure 12: The relationship between $\delta^{15}N$ and dissolved oxygen concentrations for the 2005 sample set.

Figure 12 shows a very pronounced inverse relationship between nitrate $\delta^{15}N$ values and dissolved oxygen levels in individual ground water samples. This suggests that the process of

de-nitrification under increasingly anoxic conditions of dissolved nitrate, itself formed by mineralisation under oxic conditions, may to a considerable extent be responsible for the high nitrate $\delta^{15}N$ values observed. This also suggests the presence of organic solutes, or dissolved organic carbon (DOC) in the ground water, a potability factor that should be investigated further. The case of a single borehole (Koekoek1) is discussed in the next section. The range of $\delta^{15}N$ values at low dissolved oxygen contents suggests that the organic carbon content of the ground water is variable. Such factors seem to underlie the lack of correlation between $\delta^{15}N$ and nitrate concentration (Figure 11).

4.9 Koekoek 1 borehole

This borehole is situated some 30m from a dwelling house next to a sheep enclosure on sloping terrain on the edge of a granite outcrop with thin soil cover. It was being used as a drinking water supply when sampled (TN 17) in 2005, although at that stage the NO_3-N concentration was 20 mg/ℓ, i.e. well above the potable range. The $\delta^{15}N$ value was +8.1‰ and the dissolved oxygen 1.8 mg/ℓ. These figures did not suggest major anthropogenic impact.

When the borehole was re-visited in late 2007 (TN 75), it was being used for garden irrigation only. Two pit latrines had been installed some 30 m up-slope from the borehole. They had been excavated partially by blasting into solid rock a year before. The borehole water had an unpleasant smell and appearance. As a result, no wellhead observations were made and a sample was taken for chemical analysis only.

The major ion analyses for 2005 and 2007 are compared in Table 4. There was no measurable NO_3 in the 2007 sample. All other ion concentrations had increased, the most marked being TAlk. Si had remained unchanged suggesting strongly that the chemical changes were not associated with water/rock interactions. A bacteriological analysis showed a total coliform bacteria count of 26000/100mℓ and faecal coliform at 300/100mℓ. The deterioration of water quality can therefore be linked directly to sewage pollution that resulted in increased dissolved organic carbon, probably leading to anoxic conditions and complete denitrification of NO_3.

This is an example of how a low concentration of NO_3, or its absence, may not, in itself, indicate the absence of sewage pollution.

Table 4; Comparison of major ion chemistry of Koekoek 1 borehole as measured in 2005 and 2007.

Year	pH	NO_3-N	F	TAL	Na	Mg	Si	SO4	Cl	K	Ca	EC
2005	7.99	20.3	0.21	360.3	191.6	70.1	37.5	45.0	306.2	11.7	88.4	192
2007		0.0	0.1	537.0	200	88.3	37.4	48.8	435.1	15	115	

Concentrations in mg/ℓ.

5. Preliminary conclusions regarding nitrate sources for Bochum ground water

The discussion of the isotope and other analytical data presented above has thrown some light on the ground water hydrology and hydrochemistry of the Bochum area. In particular, isotope data was able to elucidate certain aspects of the systematics of nitrate production in the area and suggests that animal and human waste contamination is probably only one source of

medium to high nitrate levels. On the other hand the degree of denitrification observed suggests fairly ubiquitous presence of dissolved organic material in ground water that might indicate diffuse pollution. It suggests further that nitrate *concentration* may not, in itself, be a reliable, or even useful, measure of anthropogenic pollution of ground water.

Results from the Taaibosch study (Verhagen et al. 2004a,b) in a very different hydrogeological setting, and a similar incidence of high nitrate concentrations, showed quite conclusively that most of these instances were of non-anthropogenic origin. This study draws a similar conclusion The outlines of a possible regional approach to the problem of ubiquitous high nitrate values in Limpopo Province can possibly be discerned in the results of both Phase I (Appendix 1) and Phase II (this report) of the investigation.

This study has shown that a combination of hydrochemistry and environmental isotope analysis can contribute significantly to an understanding of the genesis of nitrate in ground water in the context of its hydrology and hydrochemistry. The very limited number of nitrogen isotope analyses that could be produced has demonstrated that $\delta^{15}N$ data are fundamental to this, when interpreted in the framework of the overall hydrological and hydrochemical information.

Results from ^{222}Rn measurements could not be interpreted in terms of any other measured parameters or geological or physiographic associations.

In comparing the results from the Bochum study with those obtained at Taaibosch, the following may be observed:

1. The category of high ^{14}C/low ^{3}H values that was ascribed to the transport of recent biogenic carbon to the water table by phreatophyte roots at Taaibosch is much less prominent in Bochum (see Figure 1)
2. The category of ^{14}C/ ^{3}H values that plots well below the exponential model fits to the Taaibosch data, interpreted as a mixture of distinct water types, is totally absent at Bochum
3. There is a similar striking correlation between NO_3 and dissolved silicon concentrations such as observed at Taaibosch
4. The significant correlation between $\delta^{15}N$ and dissolved oxygen, taken as a measure of de-nitrification at Bochum, was not observed at Taaibosch.

The differences referred to above are ascribed to differences in geology, areas, the most fundamental being the absence in Bochum of the basalt aquifer that overlies what has been shown to be a highly-productive Karoo-sandstone, shown to control the hydraulics at Taaibosch.

6. Recommendations

1. Environmental isotope techniques should be used much more widely than at present in both ground water resource and ground water quality assessment
2. It is imperative that a functional facility for nitrogen isotope analysis be re-established, based on present state-of-the-art methodology. A mechanism to achieve this might be for the WRC to advertise a solicited project to be undertaken by a group with appropriate IRMS infrastructure and the capacity to both develop and then bring into routine operation an analytical facility for $\delta^{15}N$ analysis in water.

3. As the basalt aquifer seems to provide a specific environment for the development of high nitrate concentrations it is recommended that another look be taken at e.g. the nitrate problem on the Springbok Flats with special reference to the particular properties of the (Karoo) basalt aquifer (Heaton 1985).

7. Acknowledgements

The authors wish to thank the Water Research Commission for its support in granting a research contract for this study. The infrastructural support and hydrochemical analyses provided by the Department of Water Affairs and Forestry are gratefully acknowledged. A special word of thanks is due to the Environmental Isotope Laboratory of iThema LABS (Gauteng) for performing the isotope analyses.

8. References

Clark and Fritz (1997) Environmental isotopes in hydrogeology. Lewis, New York.

Geocon (1997) Department: Water Affairs and Forestry Refurbishment Programme in Bochum/My darling TLC. Prepared by Geocon CC in Pietersburg/Polokwane, South Africa.

Heaton, T.H.E. (1984) Sources of the nitrate in phreatic ground water in the western Kalahari. *J Hydrol* 67:249-259,

Heaton, T.H.E. (1985) Isotopic and chemical aspects of nitrate in the ground water of the Springbok Flats. *Water SA* 11:199-208, 1985.

Marais (1991). Written communication. Department: Water Affairs and Forestry, Mmabatho, Bophotatswana.

Stadler, S. (2006) Investigation of natural Processes leading to Nitrate Enrichment in Aquifers of semi-arid Regions. PhD thesis, Univ Karlsruhe, 238p.

Talma A.S. and Tredoux G. (2005). Isotopic source identification of nitrate in the ground water of semi-arid southern Africa, In: Environmental Geology in Semi-Arid Environments (Eds H Vogel and C Chilume), 92-102, Department of Geological Survey, Lobatse, 289p. ISBN 99912-0-501-2.

Taussig D.M and Verhagen, B.Th. (1991) Nitrogen isotopes act as nitrogen pollution indicators of ground water in Venda. Biennial Ground water Convention: Ground water quality and pollution, paper No. 31, Midrand, 20-23 August.

Tredoux G., (1993) A preliminary investigation of the nitrate content of ground water and limitation of the nitrate input. Report No: 368/1/93, WRC.

Verhagen, B.Th., Geyh, M.A., Froehlich, K. & Wirth, K. (1991) Isotope hydrological methods for the quantitative evaluation of ground water resources in arid and semi-arid areas. - Development of a methodology. Research Reports of the Federal Ministry for Economic Cooperation of the Federal Republic of Germany. Bonn.

Verhagen, B.Th., Butler, M.J., Van Wyk, E. and Levin, M. (2004a) A multi-tracer study of the origins, systematics and hydrologica linkages of high nitrate concentrations in ground water in Bochum District, Limpopo Province. Progress report to the WRC on project T5/1823.

Verhagen, B.Th., M J Butler and E van Wyk (2004b) Isotopes and chemistry suggest natural processes for high nitrate in Limpopo Province ground water. Extended abstracts, WISA 2004 Conference, Cape Town.

Verhagen, B.Th., M.J.Butler & E.van Wyk (2005). South African studies suggest natural production of high rural ground water nitrate and ecological links. (Abstract) Procs: International Conference: Multifunctionality of Landscapes p. 85 Justus-Liebig University, Giessen, Germany.

Verhagen, B.Th., Talma, A.S., Weaver, J. and Butler, M.J. (2008) A cooperative groundwater resource assessment with environmental isotopes in the Table Mountain Group aquifers, South Africa. Submitted: Ground Water.

Weaver, J.M.C. (1992) Groundwater sampling, a comprehensive guide for sampling methods. Report no. TT54/92, Water Research Commission, Pretoria.

WHO (1995) World Health Organization. Health hazards from nitrates in drinking water. Copenhagen, 102p.

APPENDIX 1

EXCERPTS FROM THE FINAL REPORT TO THE IAEA (2002) ON THE SOUTH AFRICAN NATIONAL PROJECT UNDER RAF/08/029 REGIONAL PROGRAMME ENTITLED:

Environmental isotope studies as part of a rural ground-water supply development : Taaibosch area, Limpopo Province, South Africa

B Th Verhagen, M J Butler, E van Wyk and M Levin

1. PROJECT RESUMÉ

The initial approach was directed by a hydrological model devised nearly ten years before, during an investigation (Fayazi and Orpen, 1989) into the feasibility of a ground water supply to a large number of villages in the Bochum District of Limpopo Province, South Africa (Fig.1). This model proposed that ground water recharged by rain to a featureless plain of some 700 km^2 in extent, drains northwards, away from the mountain watershed of the Blouberg, mainly through a shallow basalt aquifer (Fig. 2 & 3). The Tshipise fault in the north would act as a sink as well as a drain of ground water westwards towards an ephemeral river course. Initially, the underlying Karoo sandstone, encountered mainly in test drilling of upthrown blocks along and north of the fault zone, was found usually to be poorly yielding and not regarded as a worthwhile target for further exploration (see Section, Fig. 2).

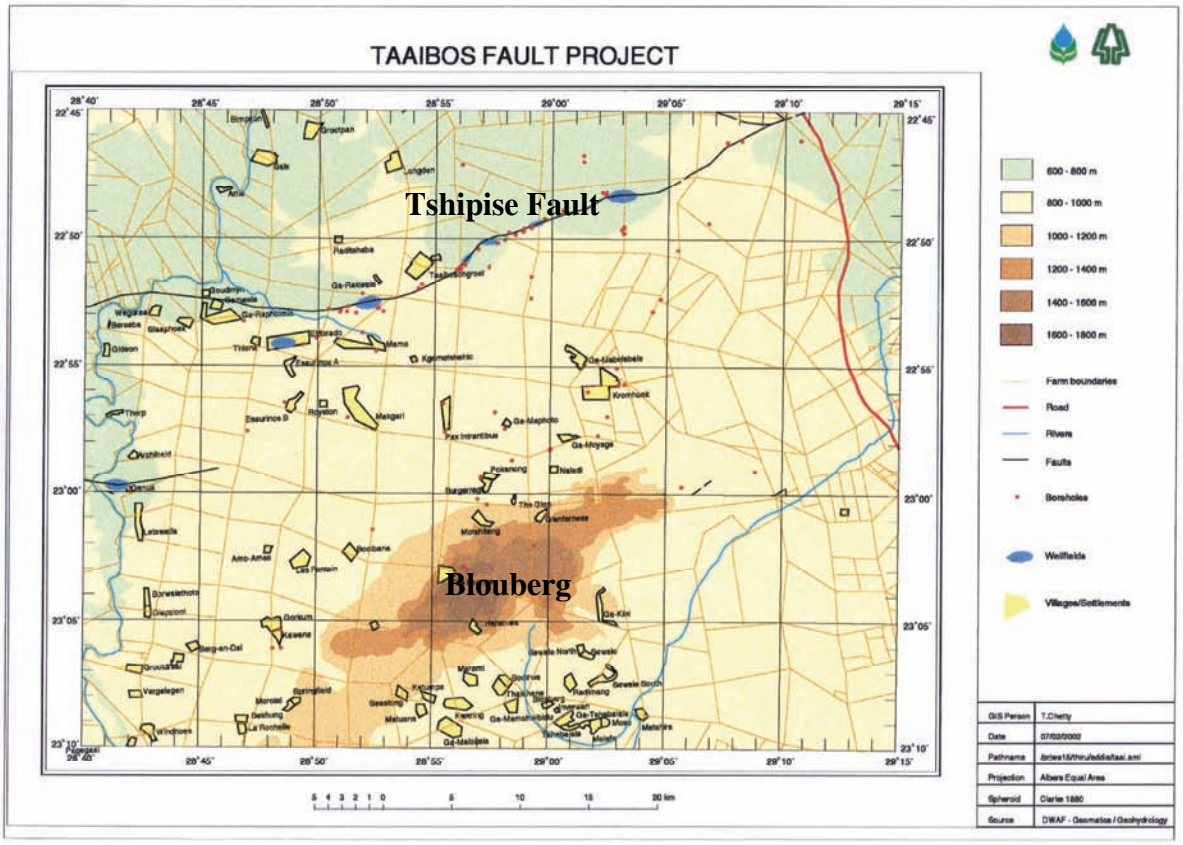

Figure 1: Topographical map of the area of study, showing villages, farm boundaries, borehole positions, the Tshipise fault and well field

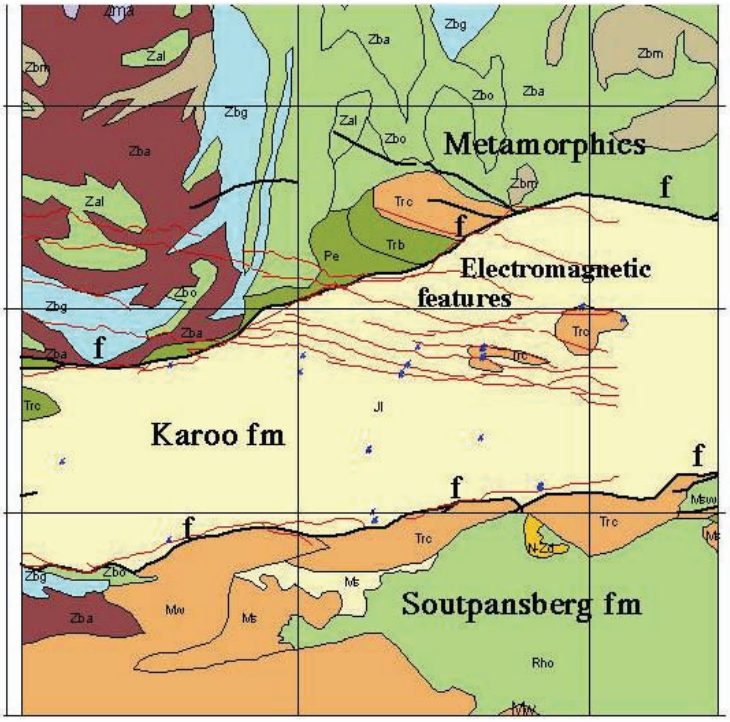

Figure 2: Schematic geology of study area, showing graben structure and electromagnetic features, faults partially intruded by dykes

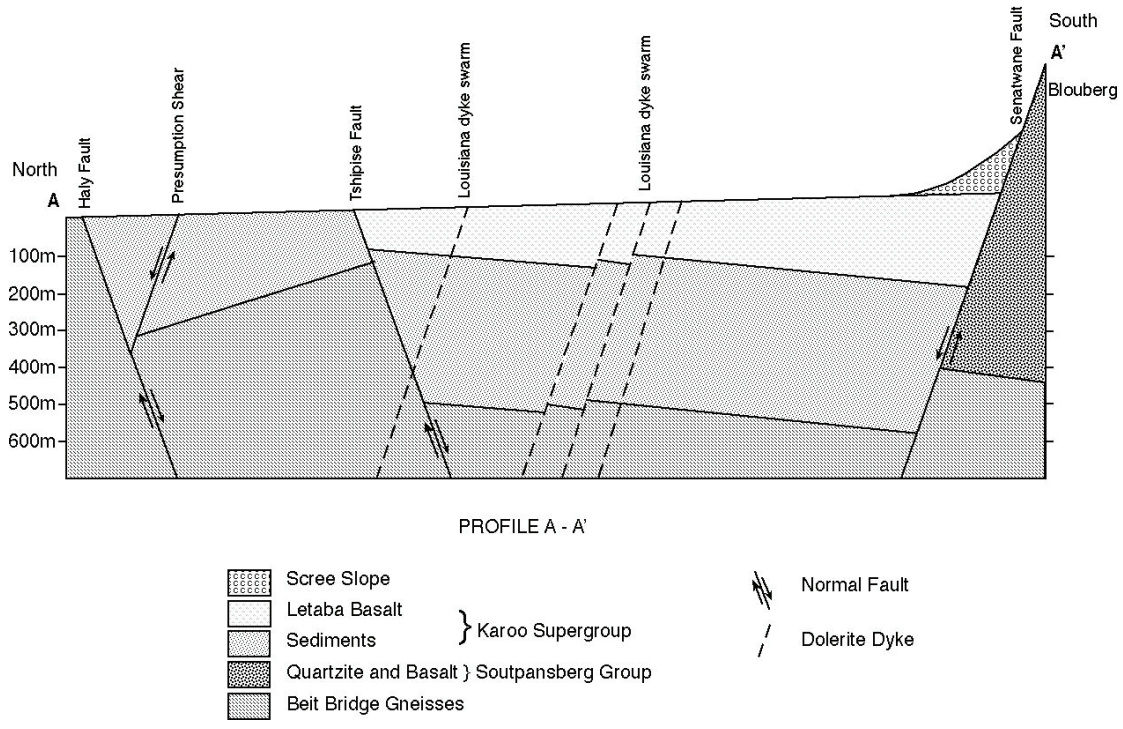

Figure 3: Schematic N-S section based on latest geological and structural information. The area of study lies between the Tshipise fault in the north to the Senotwane fault in the south.

The isotope and hydrochemical investigation focused initially on the fault zone. Stimulated partly by the isotope investigation, contract drilling both on the western and eastern sections of the fault began to reveal greater complexity of the fault structure than initially believed. Stable

isotope data show that recharge conditions in the area are fairly uniform, with a degree of surface ponding, producing a moderate evaporation imprint on the groundwater data.

An exponential mixing model for a phreatic aquifer was used to fit a plot of radiocarbon against tritium values in terms of mean residence times. Recharge rates were calculated on the basis of mean residence times derived from isotopic data, depth of saturation and estimates of aquifer porosity. An optimistic isotope-based assessment of diffuse recharge to the plain and the fault zone suggests that the earlier study over-estimated sustainable yield for the fault zone by an order of magnitude. This sounded a word of caution in terms of the development of a regional water supply.

A hydrochemical model encompassing this data suggests that sources other than the vadose zone are introducing ^{14}C into ground water. Statistically, ^{14}C provides a biased estimate of residence times, which have to be constrained mainly by the very limited range of tritium concentrations. Down-the-hole video observations revealed the highly anisotropic nature of the void space in the basalt, and widespread calcification of fractures.

It was particularly the isotope data which first led to a realisation that the area was (hydro)geologically far more complex than originally believed. This prompted a low-level airborne magnetic survey, the results showing numerous features, till then poorly known, such as lineaments intersecting the fault, which could well cause partial compartmentalisation of the aquifers. The results of this survey in turn guided a drilling programme, the results of which fed into a revised geological model and section of the area.

Several boreholes drilled in Karoo sandstone *below basalt* gave increasing blow-yield of good quality water from first strike down to final depth. The sandstone appears to have significant primary porosity. Radiocarbon shows low but active turnover of water over considerable aquifer thickness. A significant and dynamic ground water resource is being identified in the sandstone, of which the basalt aquifer, which has mainly been targeted thus far, only represents a fraction.

The principal achievements thus far of the isotope-based study of the Taaibosch area have been:

- More conservative estimates of recharge to the basalt which sound a warning on the exploitable resource of this aquifer
- Showing that the Tshipise fault zone does not constitute a regionally coherent regional drain of ground water
- The occurrence of high ^{14}C–low ^{3}H cases which point towards the transport of contemporary CO_2 to depth in the saturated zone
- The construction of a largely self-consistent hydrochemical/ecological model which may explain the high nitrate levels endemic in the area
- Prompting a more intensive geophysical and geological investigation which revealed numerous geological features which have profound hydrogeological implications
- Deeper exploratory drilling conducted during this investigation revealed substantial yields of good quality water from the sandstone below basalt which initial isotope data shows to be actively recharged
- The sandstone may in future constitute the main ground water resource in the area and could act as the target for a future regional water supply, provided it is carefully managed
- Further work in the study area will encompass :

1. determining the extent of the productive sandstone aquifer and quantifying its sustainable resource, especially associated with various structures (secondary porosity and hydraulic conductivity).
2. further investigation of the proposed mechanism of root respiration/decay to explain the apparent uncoupling of radiocarbon and tritium values
3. developing a consistent model of nitrate production in the area and possible strategies for mitigation of the problem of high nitrate concentrations.

- Points 2 and 3 will form the main thrust of the present study under WRC contract.

2. DISCUSSION OF ISOTOPE DATA

2.1 Deuterium and oxygen-18

Figure 4 shows a $\delta D - \delta^{18}O$ plot for samples from individual major rainfall events and monthly composites at the three rainfall collection stations from late 1998. The least-squares fit to this data set is $\delta D = 8.17\ \delta^{18}O + 13$. The wide range ($\delta^{18}O$~11 ‰) of values in individual rainfall events and episodes could produce significant differences in ground water stable isotope values. The relatively tight clustering in ground water values illustrates the integrative and thus smoothing effect of the recharge process in this environment.

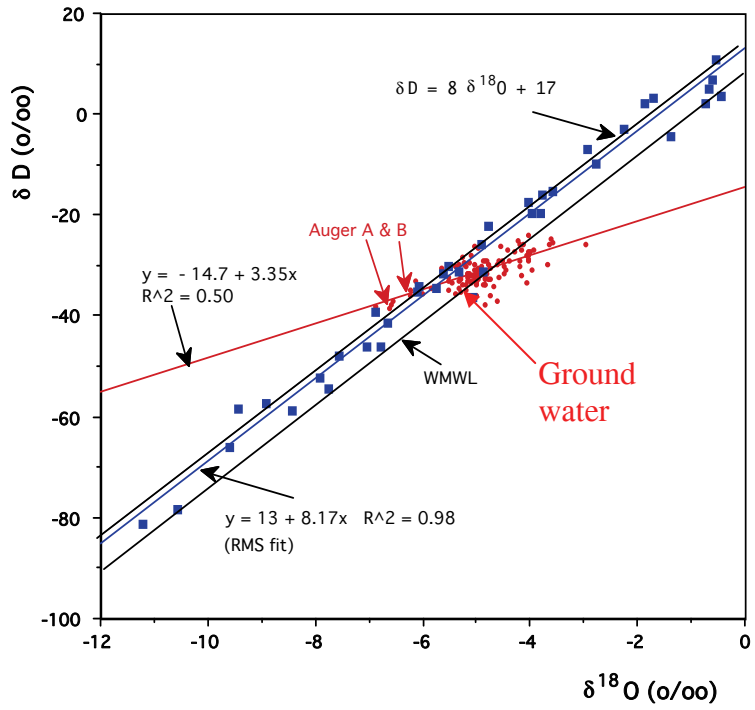

Figure 4: $\delta D - \delta^{18}O$ plot of a) rain water, with least squares fit to data , WMWL and possible LMWL b) ground water, with least squares fit.

Runoff from the Blouberg infiltrating into the extensive northern scree slopes (Fig.3) has been regarded as a likely source of recharge to the aquifers of the Taaibosch study area. The isotopic characterisation of seepage into a perennial wetland at the foot of the mountain should represent an integrated sample of infiltrated runoff over time - Auger A and Auger B (Figure 4). These clusters are the isotopically lightest of all ground water samples and fall on a proposed local meteoric water line.

Some evaporation should occur before infiltration from surface, probably as a result of ponding in numerous depressions and small pans which characterise most of the plain of the study area. The fact that very light stable isotopic values are found locally along the Tshipise fault, suggests that deeper sandstone ground water, recharged near the Blouberg, moves northwards under (semi-)confined conditions, and leaks into the basalt along the fault. This isotope model has recently found confirmation when such upwards leakage was demonstrated in individual boreholes.

2.2 Carbon-13

Figure 5 shows a plot of $\delta^{13}C$ values against ^{14}C for the entire study area. $\delta^{13}C$ values generally become more positive with increasing ^{14}C. This is opposite to the trend for e.g. a closed, confined flow system, where increasing age (decreasing ^{14}C) is accompanied by progressive carbonate development and isotope exchange producing increasing $\delta^{13}C$ values (Gonfiantini et al. 1998).

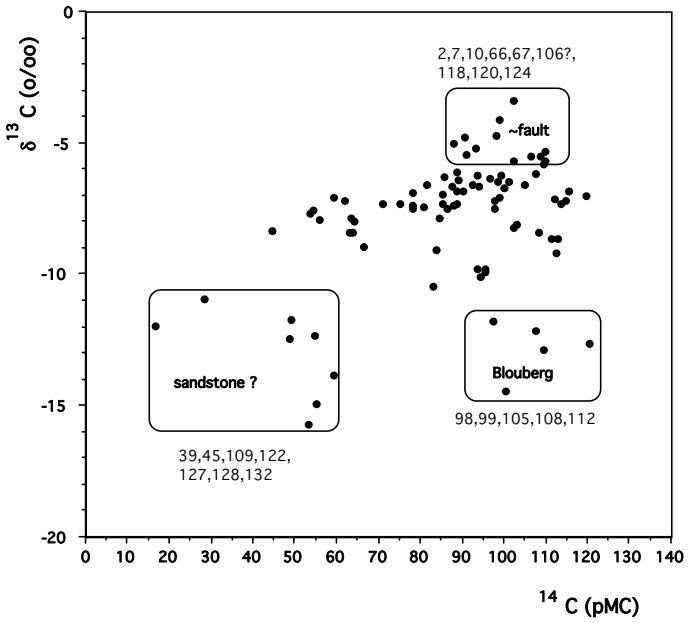

Figure 5: Plot of $\delta^{13}C$ against ^{14}C for all ground water . Also shown are a few, mainly geographical, categories.

2.3 Tritium and radiocarbon

Ground water tritium concentrations range from 0.2±0.2 TU (the limit of detection) up to 5.6±0.3 TU. Radiocarbon values range from 16.5 – 120.3 pMC.

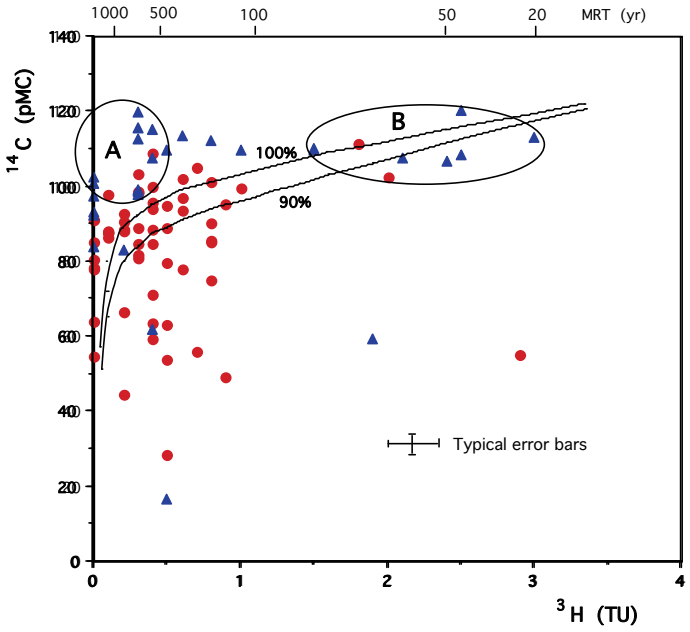

Figure 6: Plot of ^{14}C against ^{3}H values before (circles) and after 2000 (triangles) and exponential model plots for 100% and 90% atmospheric ^{14}C.

Figure 6 shows a plot of all ^{14}C against ^{3}H values. The solid lines are the locus of pairs of values of ^{14}C and ^{3}H for different mean residence time (MRT) values, shown along the top of the diagram. The lines are, respectively, for ^{14}C recharge values at 100% and 90% atmospheric. Tritium, a conservative tracer of water, can therefore act as a constraint in estimating the initial - or recharge - value of potentially non-conservative radiocarbon. Values on or near the lines in Figure 6 are taken as conforming to phreatic aquifer behaviour. Many radiocarbon values $\geq$ 95 pMC accompanied by tritium >1TU (recent recharge) fall in this Category (B). Values significantly below the lines may be interpreted as mixtures of more recent (higher ^{3}H) water at low alkalinity, with older (lower ^{14}C), higher alkalinity water. These are possibly hydrological mixtures. Points above the line imply a mechanism through which radiocarbon (solute) has moved more rapidly than the solvent (ground water) – hydrologically a "forbidden zone".

Many radiocarbon values $\geq$95 pMC in ground water, which are here ascribed to post-1963 (thermonuclear) recharge, are accompanied by tritium values at the limit of detection (Category A). This phenomenon has been encountered in other environments, especially in igneous terrains (Verhagen, unpub. data).

Various processes may be operative in the development of the TDIC in the area. The 'standard' model applies, in which the TDIC production is completed largely in the vadose (soil) zone, producing ^{14}C values close to atmospheric and $\delta^{13}C$ values, reflecting the photosynthetic pathway of the plant material. Liberation of CO_2 by tree roots would keep the DIC of the saturated zone in their vicinity close to the atmospheric radiocarbon value, independent of the recharge process. Ongoing leaching by tree root CO_2 could lead to calcite supersaturation and precipitation of calcite, which in turn would partly be re-mobilised. This ongoing cyclical process could produce more positive values of $\delta^{13}C$ values in TDIC in association with high ^{14}C (Figure 6).

Static water levels in the area of study are generally shallow, ranging from 7 – 40 metres with an average of ~15 m. A common tree in the area is Acacia erioloba (camel-thorn tree), a known phreatophyte, amongst others. There is anecdotal evidence, as well as information obtained by excavation (M.Scholes, priv. comm.), of substantial structural roots found at

depths of tens of metres in similar environments. Root respiration could transport radiocarbon to the saturated zone more rapidly than tritium, which labels the infiltrating rain water. Brandl (2002) reports marked stratification in the basalt, more weathered layers alternating with fresher, less permeable material. In addition, sharp differences of water level across dykes of the dyke swarm in the N and NE have shown that dykes act as ground water barriers, further compartmentalising sections of basalt vertically. Tree roots may well tap such more permeable compartments, which would be partially isolated both vertically and horizontally. Some of the cases lying in the "forbidden" Zone A are found in this area, generally in boreholes with low yield.

2.4 Radon

Radon values span a range of 0 – 1515 cpm/ℓ and are relative activities only. The highest activity may be influenced by coal-bearing Karoo sediments in the area. Very little correlation with lithology, structure or hydrochemistry could be observed. When plotted against both tritium and radiocarbon (Figure 7) it is observed that there is a trend of increasing radon with increasing ^{14}C and decreasing ^{3}H respectively.

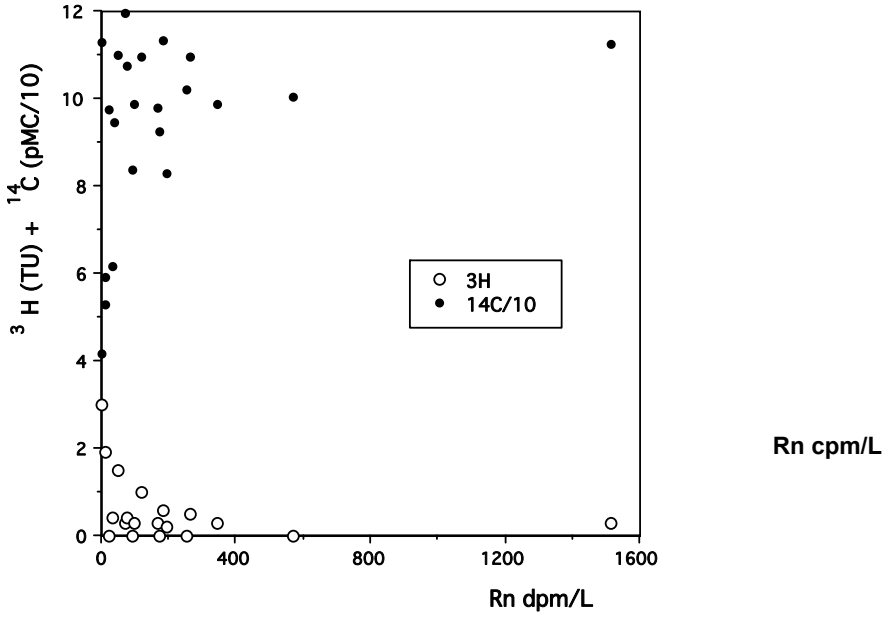

Figure 7: Plot of ^{3}H and ^{14}C (pMC/10) values against ^{222}Rn.

Low tritium values accompanying clear cases of thermonuclear radiocarbon ("forbidden Zone A") have been tentatively explained as the result of respiration of CO_2 by deep (tree) roots. This renewed acidity in ground water would re-activate weathering of basalt aquifer minerals at depth. The radon correlations with ^{3}H and ^{14}C could be interpreted as supporting such weathering in that radon would be more readily released from the rock where it is actively being eroded.

3. TOWARDS AN UNDERSTANDING OF THE HYDROCHEMICAL DEVELOPMENT OF GROUND WATER IN THE TAAIBOSCH AREA

3.1 Renewed hydrochemical development

A model explains "forbidden" cases (A) of radiocarbon values much higher than can accompany low to vanishing tritium. Root respiration of CO_2 assimilated by trees from the atmosphere would transport ^{14}C more rapidly than tritium through infiltrating ground water. A

consequence is that hydrochemical reactions, which would normally be completed in the vadose zone, may be re-activated at the depth of tree root systems.

The Karoo basalt contains plagioclase with various proportions of albite and anorthite. Renewed acidity from the generation of CO_2 decomposes these minerals to clay (kaolinite) and liberates cations and dissolved silicon:

$$NaAlSi_2O_8 + H^+ + 9/2H_2O = 1/2Al_2Si_2O_5(OH)_4 + Na^+ + 2Si(OH)_4$$

$$CaAl_2Si_2O_8 + 2H^+ + H_2O = Al_2Si_2O_5(OH)_4 + Ca^{2+}$$

The ongoing production and remobilisation of calcite was invoked to explain a rising trend in $\delta^{13}C$ with increasing ^{14}C. The model could have other chemical and isotopic consequences.

The Si concentration in ground water is a measure of feldspar decomposition. It can therefore be expected that Si concentration will increase with increasing ground-water residence time. The generally positive correlation trend of Si with ^{14}C concentration in the study area (Figure 8) - on the face of it the inverse of the above - suggests that feldspar decomposition is occurring in zones of higher biogenic CO_2 input. Such high input is conventionally the vadose zone. According to the model, this could also occur in less well leached zones through root respiration of CO_2. Limits on Si concentration are its solubility and ongoing, if possibly periodic, ground water turnover. There is no significant correlation of Si with ^3H.

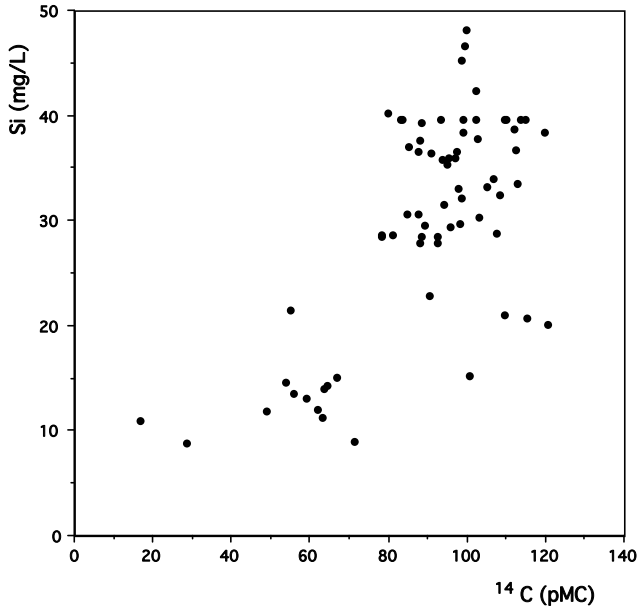

Figure 8: Plot of Si (mg ℓ^{-1}) against ^{14}C

Concentrations of NO_3-N in excess of 10 mg/ℓ (WHO maximum allowable level for potable water) are common in the study area (Fig. 9). The majority of the sampled boreholes are situated away from human habitation and cattle concentrations. It is therefore plausible that much of the high nitrate observed has a natural, rather than anthropogenic, source.

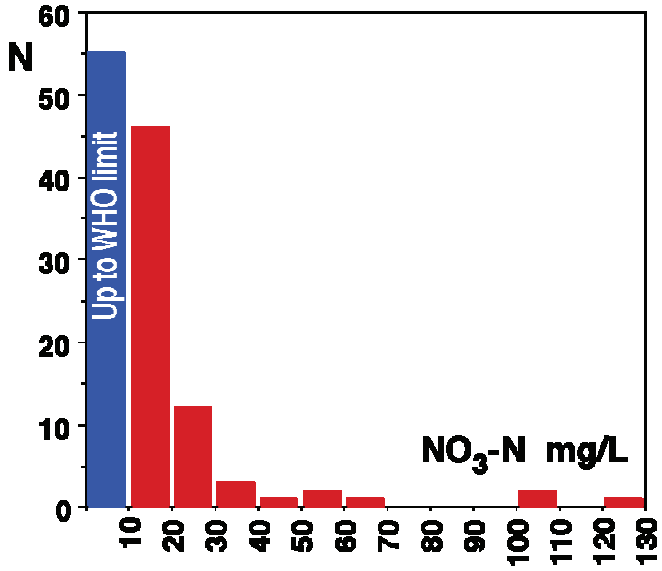

Figure 9; Frequency histogram of nitrate concentrations in ground water samples from boreholes in the Taaibosch area.

Concentrations of NO_3-N >10 mg/ℓ and ranging up to 190 mg/ℓ are associated with radiocarbon values >80 pMC (Figure 10). However, not all nitrate values in this range of radiocarbon values are elevated.

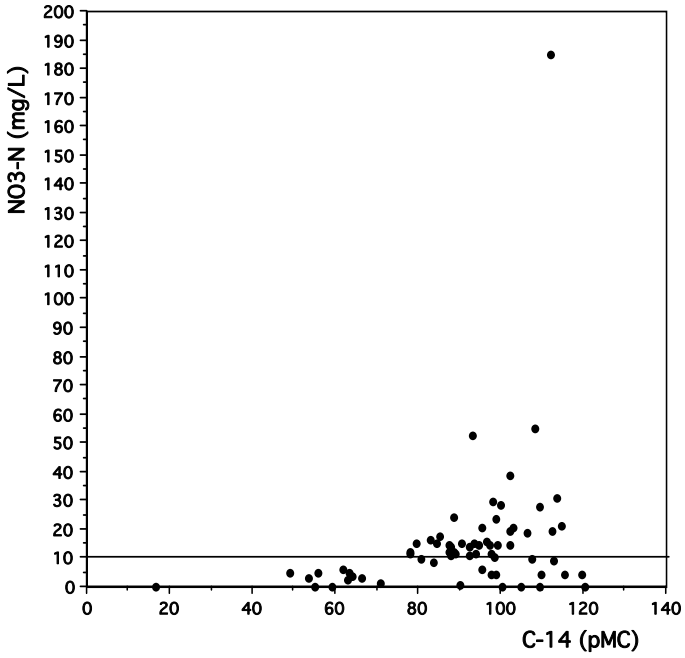

Figure 10. Plot of NO_3-N (mg ℓ^{-1}) vs ^{14}C.

There is little correlation of nitrate with ^{3}H (Figure 11). Most of the results are for values <1 TU, even for NO_3-N values >10 mg/ℓ. This behaviour is largely opposite to the correlation with radiocarbon. On the other hand, some of the highest values correspond to tritium values > 1 TU. These are interpreted as cases of active, ongoing recharge. Vadose zone processes, and possible anthropogenic sources, are therefore also effective in nitrate production in the area.

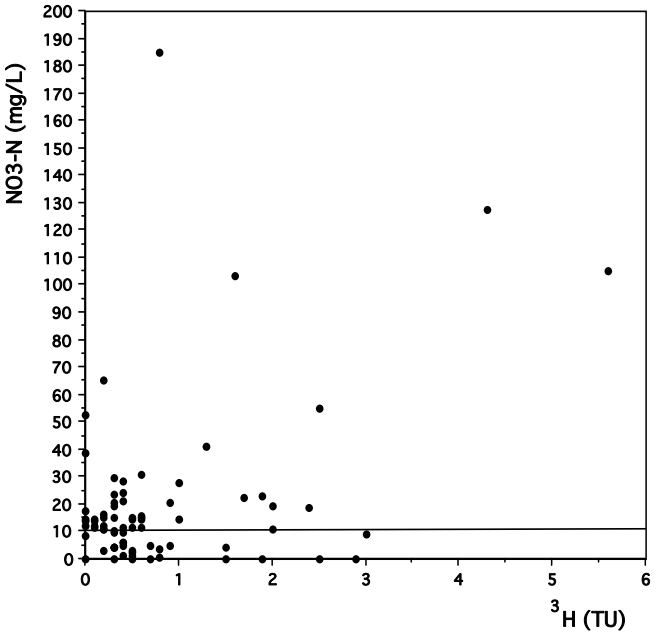

Figure 11. Plot of NO_3-N (mg ℓ^{-1}) vs ^3H.

Most of the NO_3-N values >10 mg/ℓ correspond to Si values >30 mg/ℓ (Figure 12). It would appear that the generation of NO_3 is concomitant with the dissolution of Si, which further strengthens the conclusions arrived at above.

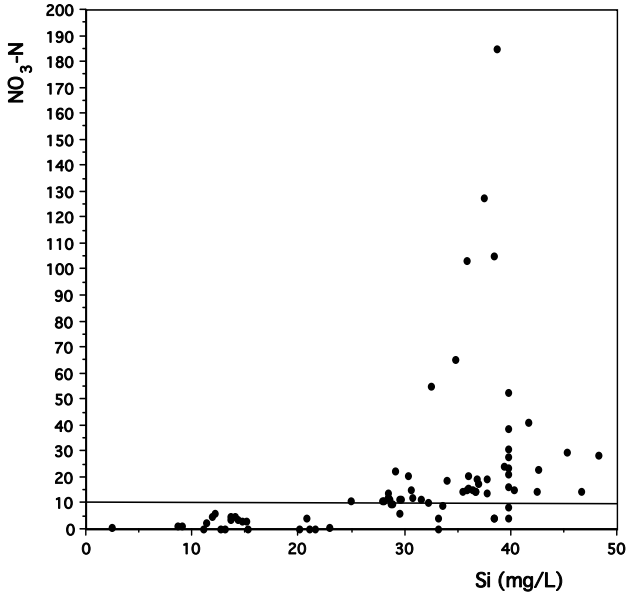

Figure 12. Plot of NO_3-N (mg ℓ^{-1}) vs Si (mg ℓ^{-1}).

3.2 Towards an isotope/nitrate model.

A possible model which presents itself is based on "excess" radiocarbon at depth which is unassociated with ^3H. Deep roots of phreatophyte acacia and other nitrogen-binding trees which abound in the area liberate CO_2 by root respiration as well as by the decomposition of discarded active small or *functional* roots (M. Scholes priv. comm.) This CO_2 reacts with rock minerals on an ongoing basis and facilitates the liberation of ^{222}Rn. The observed correlation of ^{222}Rn with ^{14}C and an apparently opposite trend with ^3H, supports the mechanism.

This process keeps the ^{14}C in TDIC close to the prevailing atmospheric value, reduced by a 'dilution factor' (~0.9). The concentration of TDIC is buffered by supersaturation and the production of secondary calcite. Down-the-hole video monitoring has shown extensive calcification of smaller fractures in the basalt all the way down the saturated zone. The secondary calcite in turn can be re-mobilised, this re-cycling raising the $\delta^{13}C$ values in TDIC. High ^{14}C concentrations in association with tritium >1 TU indicate areas of active recharge and phreatic flow. The many cases of tritium $\leq$0.5 TU indicate turnover or residence times >200 years and more-or -ess isolated aquiferous zones.

The fact that Si positively correlates with ^{14}C and not with ^{3}H suggests that high Si concentrations do not result from evapotranspirative enrichment in the soil zone, but are the product of weathering at depth. Nitrate-N values are positively correlated with ^{14}C and Si. This supports the model that, along with CO_2, organic nitrogen is liberated by the seasonal decay of discarded functional roots.

Drilling records often indicate only one significant water strike in the basalt. These coincide with major cavities, as seen in down-the-hole video images. More uniform water-bearing and transporting properties are suggested by a wider spread of smaller pores, joints and fractures, which are, however, often cemented. Prawn-like aquatic fauna (amphipoda) seen in video images of several boreholes are associated with macropores, probably regionally connected. Amphipoda reveal the presence of nutrients and of oxic ground water, allowing decay-produced nitrogen to be oxidised to nitrate.

4. REFERENCES

Brandl, G. 2002. Summary of the preliminary report on the project: Construction of a geological-structural model for the Tshipise Fault Zone in the Alldays area, District Bochum, Northern Province.

Fayazi, M. & Orpen, W.R.G. 1989. Development of a water supply for Alldays from groundwater resources associated with the Taaibos fault. Techn. Rep. GH 3664, Department of Water Affairs and Forestry, Pretoria.

Verhagen, B.Th., Geyh, M.A., Froehlich, K. & Wirth, K. 1991. Isotope hydrological methods for the quantitative evaluation of ground water resources in arid and semi-arid areas. - Development of a methodology. Research Reports of the Federal Ministry for Economic Cooperation of the Federal Republic of Germany. Bonn.